

Review

Environmental Reservoirs of *Vibrio cholerae*: Challenges and Opportunities for Ocean-Color Remote Sensing

Marie-Fanny Racault ^{1,2,*} , Anas Abdulaziz ³ , Grinson George ⁴, Nandini Menon ⁵, Jasmin C ³, Minu Punathil ⁴ , Kristian McConville ¹, Ben Loveday ¹, Trevor Platt ^{1,4}, Shubha Sathyendranath ^{1,2} and Vijitha Vijayan ⁴

¹ Plymouth Marine Laboratory, Prospect Place, The Hoe, Plymouth PL1 3DH, UK; krm@pml.ac.uk (K.M.); blo@pml.ac.uk (B.L.); tplatt@dal.ca (T.P.); ssat@pml.ac.uk (S.S.)

² National Centre for Earth Observation (NCEO), Plymouth PL1 3DH, UK

³ Council of Scientific and Industrial Research (CSIR)-National Institute of Oceanography (NIO), Regional Centre, Abraham Madamakal Road, Cochin, Kerala 682 018, India; anas@nio.org (A.A.); jasminc@nio.org (J.C)

⁴ Indian Council of Agricultural Research (ICAR)-Central Marine Fisheries Research Institute (CMFRI), Abraham Madamakal Road, Kochi 682 018, India; grinson.george@icar.gov.in (G.G.); minu.punathil@gmail.com (M.P.); vijithavijayan85@gmail.com (V.V.)

⁵ Nansen Environmental Research Centre India (NERCI), First floor, Amenity Centre, KUFOS, Kochi, Kerala 682506, India; nandinimenon@nerci.in

* Correspondence: mfrt@pml.ac.uk; Tel.: +44-175-263-3434

Received: 4 October 2019; Accepted: 20 November 2019; Published: 24 November 2019



Abstract: The World Health Organization has estimated the burden of the on-going pandemic of cholera at 1.3 to 4 million cases per year worldwide in 2016, and a doubling of case-fatality-rate to 1.8% in 2016 from 0.8% in 2015. The disease cholera is caused by the bacterium *Vibrio cholerae* that can be found in environmental reservoirs, living either in free planktonic form or in association with host organisms, non-living particulate matter or in the sediment, and participating in various biogeochemical cycles. An increasing number of epidemiological studies are using land- and water-based remote-sensing observations for monitoring, surveillance, or risk mapping of *Vibrio* pathogens and cholera outbreaks. Although the *Vibrio* pathogens cannot be sensed directly by satellite sensors, remotely-sensed data can be used to infer their presence. Here, we review the use of ocean-color remote-sensing data, in conjunction with information on the ecology of the pathogen, to map its distribution and forecast risk of disease occurrence. Finally, we assess how satellite-based information on cholera may help support the Sustainable Development Goals and targets on Health (Goal 3), Water Quality (Goal 6), Climate (Goal 13), and Life Below Water (Goal 14).

Keywords: *Vibrio cholerae*; waterborne diseases; cholera outbreaks; ocean-color remote sensing; Earth observation; epidemiology; ecology; microbial ecosystems; modeling; surveillance; forecast; SDGs for health; climate; water quality; oceans

1. Introduction

Vibrio bacteria are ubiquitous Gram-negative bacteria in the marine environment. These microscopic microorganisms live either in free planktonic form or in association with host organisms, non-living particulate matter or in the sediment, and participate in various biogeochemical cycles [1]. They are particularly abundant and diverse in the coastal environment, represented by more than 100 species, of which at least twelve are pathogenic. The *Vibrio cholerae* is the principal diarrheal human

pathogen, causing acute intestinal infection with watery diarrhea. There are at least 200 serogroups of *V. cholerae*, with toxigenic serogroups of O1 and O139 involved in human epidemics [2,3]. In 2017, the cholera disease was reported to affect at least 47 countries worldwide, resulting in an estimated 2.9 million cases per year worldwide [4].

Over the past decades, several programs have been initiated across the globe for continuous monitoring of microbial quality of coastal waters, such as the European Centre for Disease Prevention and Control which maps *V. cholerae* in the environment, the U.S. Holden Laboratory project on coastal microbial water quality, and the Seawater Quality Monitoring Program in India. The use of remote-sensing observations to map cholera outbreaks in relation to environmental conditions was first proposed R. Colwell in 1996 [5]. Since then, associations between satellite-derived environmental variables such as temperature, salinity, sea surface height, chlorophyll concentration, and phytoplankton abundance have been further explored and exploited to improve our understanding of the ecology of bacterial pathogens and assess the risk of various water-associated diseases at different spatial and temporal scales (e.g., [6,7]). In the case of *Vibrio* bacteria, remote-sensing observations have been used to characterize the environment in which the pathogens and their hosts thrive, and specifically with ocean-color remote sensing observations to infer key biological variables related to the dynamics of phytoplankton (a putative host for *Vibrio* bacteria).

In the coming years, the development of research programs integrating in-situ and remote-sensing observations will be key in helping to address issues related to the risk of water-borne infectious diseases for human health. In the international coordination context, the intergovernmental organization Group on Earth Observations (GEO) has been working to promote the development of such research programs and to improving the use of Earth observations to support achievement of the United Nations 2030 Agenda for Sustainable Development. The agenda sets out a collection of Sustainable Development Goals (SDGs) with associated targets and indicators around three interdependent pillars of sustainable development: economic, social, and environmental. The potential of satellite observations to help achieve the global goals is recognized across the span of social, economic, and environmental SDG indicators [8,9]. However, the specific assessment of the potential of EO to support progress in SDGs related to the risk of water-borne infectious diseases for human health, and how these may help to design research activities that minimize negative interactions between goals and maximize positive ones [10] are yet to be addressed.

Many reviews have been published in relation to disease incidence, pathogenicity, anti-microbial resistance, and persistence mechanisms of *Vibrio* bacteria, and the use of satellite-based remote-sensing observations and modeling approaches for monitoring and forecasting risks to human health, e.g., [11–18]. However, none of these reviews have specifically addressed the potential of ocean-color to study the dynamics of environmental reservoirs of *Vibrio* bacteria via the characterization of ecological and biogeochemical signatures of *Vibrio* bacteria, and how this information may be relevant to support SDGs and assess related targets and indicators.

Here, we review: (1) The interaction of *Vibrio* bacteria with the environment and with living/non-living hosts present in the aquatic system; (2) the opportunities provided by remote-sensing observations, especially ocean color, to advance our understanding of the dynamics of environmental reservoirs of *Vibrio* bacteria and improve predictability of occurrence of disease outbreaks and risks to public health; and (3) articulate how these activities provide support to SDG targets on Health (Goal 3), Water quality (Goal 6), Climate (Goal 13), and Life under the water (Goal 14).

2. Global Distribution of *Vibrio cholerae* and Cholera Disease Outbreaks

Vibrio bacteria represent a significant portion of the culturable fraction of heterotrophic bacteria in estuarine and marine waters around the world [19]. The species *V. cholerae* may colonize human populations exposed to contaminated marine waters during recreational and fishing activities, or through drinking and consumption of contaminated water or seafood respectively [20–23]. The infected persons may then carry the bacteria to different places to which they travel.

Based on genetic reconstruction from clinical data, the onset of the seventh pandemic of cholera in 1961 has been traced back to a population of *V. cholerae*, El Tor, in the north-eastern Indian Ocean basin [24]. Since then, this pandemic has spread globally. Detailed genomic analysis shows that in the Americas, the pandemic spread in three main transmission waves through pathogens introduced by human travelers: A first introduction in Latin America in 1991 of a lineage from west-Africa; a second introduction in Mexico in 1991 but this time, belonging to a lineage from Asia or Eastern Europe; and a third, more recent introduction in 2010, into Haiti, involving the import of a South Asian strain [25,26].

However, *V. cholerae* does not require a human host to survive. They form an integral part of the native flora of aquatic environments, living (1) as free-floating bacterioplankton, (2) attached to non-living particles, and (3) in a symbiotic association with a living host ([27], see Section 3). The bacteria may be transported through long-distance oceanic corridors by currents, as well as in ballast-waters from ships. The occurrence of epidemics in endemic and non-endemic countries have been shown to originate primarily in coastal regions, and then spread inland through human transportation.

The presence of *V. cholerae* serogroups O1/139 that can cause cholera disease and non-O1/139 groups that can cause gastrointestinal infections or extra-intestinal infections, such as wound infections or otitis, have been reported in European coastal waters and recreational beaches of the North Sea [28,29], Baltic sea [30]; coastal waters of America in Argentina [31], Brazil [32], Haiti [3,33], Mexico [34], Peru [35,36], Uruguay [31], Venezuela [37], United States [38], and in ballast water tanks of ships in the Chesapeake Bay [39]; coastal provinces of African countries bordering the Gulf of Guinea, including Angola, Benin, Cameroun, Cote d'Ivoire, Republic of the Congo, Guinea, Guinea-Bissau, Senegal, Sierra Leone [4], and coastal provinces of Eastern African countries including Djibouti, Kenya [40], Mozambique [41], Tanzania [4]; estuarine waters of India and Bangladesh [42–46]; as well as in coastal regions in China [47], Vietnam [48], Comoros islands, and coastal waters of the State of Papua New Guinea [4].

3. Interactions of *Vibrio cholerae* with the Aquatic Environment

This section presents aquatic reservoirs of *V. cholerae* along with the environmental processes influencing bacterial growth, mortality, virulence, and biogeochemical activity. A schematic diagram of the bacterial interaction with the environmental reservoirs is presented in Figure 1.

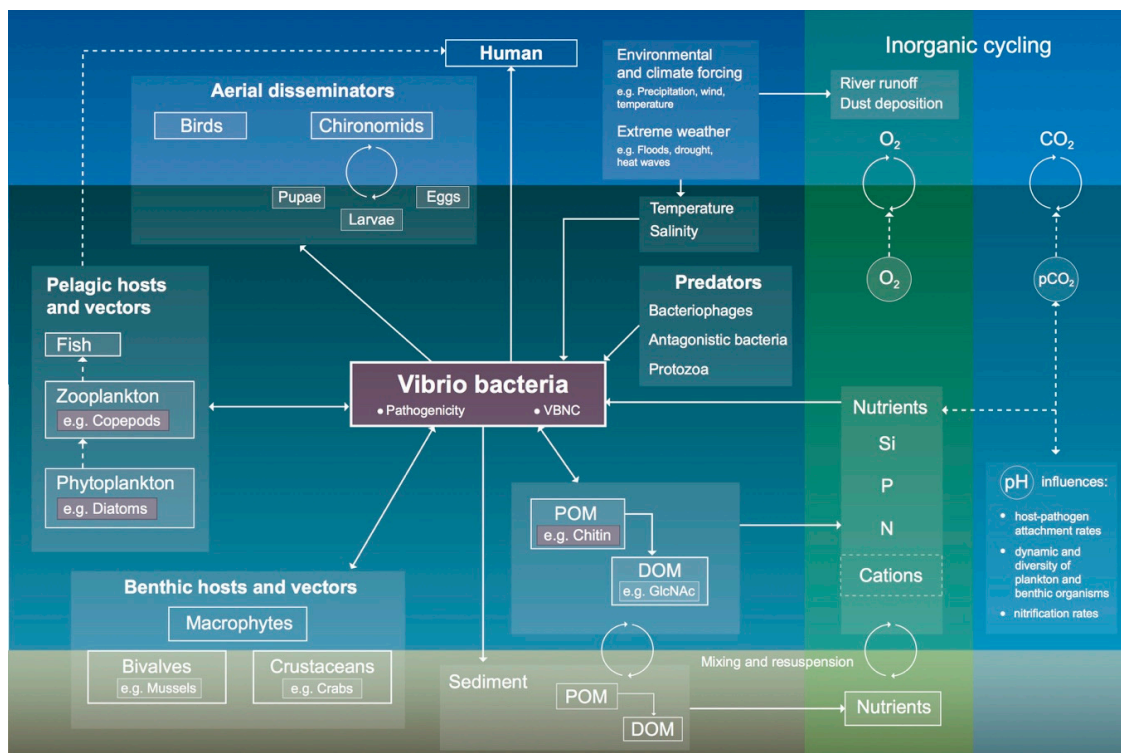


Figure 1. A schematic representation of environmental reservoirs of *V. cholerae*. The bacteria can be found as free-floating organism in the water column or interacting with various ecosystem components, including phytoplankton, zooplankton, fish, water-column and sediment particulate organic matter (POM) and dissolved organic matter (DOM), benthic organisms such as crustaceans, bivalves and macrophytes, aquatic birds, chironomids, and humans. The environmental reservoirs may support: (1) Host–pathogen interactions with a host providing a source of nutrients and protection; (2) transport mechanisms (for instance with birds and insects) allowing dissemination of the bacteria over long distances; (3) vectors of infection allowing transmission of pathogenic bacteria to human, for instance through consumption of fish or seafood or drinking of contaminated water; (4) predatory–prey interactions; and (5) biogeochemical cycling via organic matter decomposition associated with the secretion of hydrolytic enzymes by *V. cholerae*, such as chitinase that degrades chitin polymers into low-molecular-weight compounds such as N-Acetylglucosamine (GlcNAc) monomers that enter the microbial loop and can be taken up by other organisms in the ecosystem. The presence and interactions with chitin are indicated in boxes with purple color background (i.e., boxes labeled as Chitin, Diatoms, and Copepods). The influence of environmental and climate conditions is indicated, with hydrological drivers such as temperature, salinity, O₂, pH, nutrients, and cations influencing the growth, mortality, virulence, and dormancy (also-called Viable But Non-Culturable (VBNC) state). The concepts depicted in this schematic are described in the literature review presented in Sections 3.1–3.4 and in [1,15,49].

3.1. *Vibrio cholerae*: Growth, Pathogenicity, Dormancy, and Mortality

3.1.1. Growth and Abundance

The growth and abundance of *V. cholerae* are primarily controlled by temperature and salinity. This tight relationship is well established across the northern and southern hemispheres, with reports for instance in the North Atlantic and North Sea [50,51], the Chesapeake Bay [38,52], tropical riverine-estuarine environments [45], and along the coast of Peru [36]. Other environmental variables including pH, turbidity (mixing of particles), the concentrations of dissolved oxygen (DO), dissolved organic carbon (DOM), particulate organic carbon (POM), ammonium, nitrate, phosphate, silicate, iron, heavy metals, pigments, the carbon/nitrogen ratio of suspended organic particulates, the abundance of host organisms, and effects of predation by protozoans and viruses have also been reported to

affect the abundance of *V. cholerae*. However, they tend to explain a smaller fraction of the variance in *V. cholerae* abundance or the relationships between the environmental covariates and bacteria abundance may be less consistent across sites (e.g., [53–55]). These findings may also be subject to the availability of observations, availability of concurrent measurements of environmental variables and *V. cholerae* abundance, and the difficulty in detecting and measuring changes in abundance during short-term, sporadic events. For instance, an intense phytoplankton bloom was shown to stimulate fast-growth rates of *V. cholerae* population (>4 doublings per day), allowing them to overcome the grazing pressure exerted by heterotrophic nanoflagellates [56,57]. A rapid and explosive increase in *V. cholerae* abundance has also been reported in relation to the atmospheric deposition of nutrient-rich dust from the Saharan desert in surface waters of the subtropical Atlantic Ocean [58]. However, the role of dust-associated iron is controversial and other growth factors have been suggested as main drivers of *Vibrio spp.* population dynamics in response to addition of dust leachate [59].

3.1.2. Dormancy

Variations in environmental conditions such as the occurrence of a temperature outside the optimum-growth range, elevated or lowered osmotic concentrations, nutrient limitation, reduced oxygen levels, and high concentration of pollutants such as heavy metals may cause *V. cholerae* to remain dormant for a long time, i.e., viable but non-culturable status (VBNC) and regain viability once conditions become favorable [60]. The VBNC status may adversely affect cultivability and introduce a bias in forecast models designed from culture-based experiments. *V. cholerae* in VBNC status has been shown to regain its viability and pathogenicity on ingestion into the human intestine [15].

3.1.3. Pathogenicity

The pathogenicity of *V. cholerae* is controlled by the synergistic expression of different genes initiated by the transcriptional activator ToxR that leads to the production of a cholera toxin (CT) genetic element called CTX. Pathogenic strains of *V. cholerae* are evolved from environmental forms that have the ability to colonize intestines. The major virulence genes of *V. cholerae* are reported to be acquired from a lysogenic bacteriophage (CTX ϕ). Under favorable environmental conditions, other phages may cooperate with the CTX ϕ in a horizontal transfer of genes in *V. cholerae* including acquiring virulence genes from other organisms [61,62]. Coastal waters can be particularly favorable for horizontal gene transfer as divalent cations such as Ca²⁺ and Mg²⁺ present in saline waters, and metals such as vanadium, cadmium, and nickel (often found as pollutants in coastal systems), could improve the competency of bacterial cells and exert selective pressure promoting horizontal gene transfer [63].

3.1.4. Mortality

Predation by lytic phages [64], heterotrophic nanoflagellates, protozoans, rotifers, and cladocerans [14], and changes in hydrological and chemical conditions (e.g., availability of nutrients, viable temperature, and salinity conditions), are the main factors controlling the mortality of *V. cholerae* in the aquatic environment. *V. cholerae* has developed several mechanisms to survive predation and reduce pressure of hydrological stressors. Biofilm formation and morphological shift may provide physical protection to grazing by protozoans. The environmental amoeba, *Acanthamoeba castellanii*, has been reported to ingest and promote the growth of *V. cholerae* in the cytoplasm of their trophozoites and cysts [65]. Such ingestion may protect *V. cholerae* from other environmental stressors and grazing pressure. Furthermore, culture experiments [66] and epidemiological studies in coastal waters [67] suggest that control of *V. cholerae* populations may be more influenced by phage predation than by nutrient limitation. Vibriophages have also been shown to significantly influence the seasonal dynamics of cholera epidemics [61]. For instance, positive relationships have been reported between cholera incidence and the prevalence of lytic phages in the environment during the weeks preceding an outbreak in sewage waters in Lima, Peru [68], and in coastal waters of Dhaka, Bangladesh [69].

3.2. Environmental Reservoirs and Dissemination of *V. cholerae*

Sediment, as well as benthic and pelagic organisms, can form reservoirs of *V. cholerae* [15,49]. Some examples include the association of *V. cholerae* with aquatic plants [70], arthropods and chironomid egg masses [71,72], shellfish [23], waterfowl [73], fish [74,75], and planktonic and benthic organisms containing chitin, such as diatoms [76], bivalves, copepods, cladocerans, and other crustaceans [77], and aquatic sediments (e.g., [49,78]). The presence and abundance of *V. cholerae* in one reservoir may reflect a specific survival strategy of the bacteria in the environment through the attachment to organic matter, sediment particles, debris, or biofilms. However, it remains unclear whether *V. cholerae* generally predominate in one environmental reservoir over another.

3.2.1. Host–Pathogen Interactions

Attachment of *V. cholerae* to living or non-living hosts is mediated by their pili via three sets of differentially regulated genes, which also control the degradation of chitin ([79]; please see Section 3.3). Temperature, salinity, and pH have been shown to influence attachment rates of *V. cholerae* to planktonic crustaceans such as copepods by activating the expression of the Mannose-sensitive haemagglutinin (MSHA) pilus receptor and the outer membrane colonization (protein) factor GbpA [15,80]. In addition, several studies have confirmed the role of chemotaxis in chitin and the production of multiple chitinases in zooplankton–*V. cholerae* interactions [79,81–83].

The metabolic interactions of *V. cholerae* with host organisms in the marine ecosystems are diverse and may occur anywhere in a continuum between parasitism and mutualism. In many cases, the host organisms provide space and nutrients for the growth of the bacteria [15]. An example is with the dissolved organic matter secreted by phytoplankton, which has been shown to support the growth of *V. cholerae* [84]. In return, the bacteria may provide CO₂, nitrogen, phosphorus, sulfur, and trace elements to the phytoplankton.

3.2.2. Aerial-Dissemination Modes

Free-living *V. cholerae* can attach to the surface of windblown sand and dust particles from large desert areas, and to the eggs of flies that settled on hard substrates in the surface water and on the emergent adult flies [85]. Flying chironomids carrying large numbers of *V. cholerae* may be uplifted by winds into the troposphere and transport pathogens over long distances and time [85], possibly causing the occurrence of cholera outbreaks in geographically distant localities in India, Africa, and Yemen [71,72,86].

Aquatic birds, especially migratory ones, play a significant role in the transportation of *V. cholerae* via two main routes. In the first route, birds may eat contaminated fish or other contaminated organisms in one pond and shed the pathogens in another area, as demonstrated by the presence of pathogenic *V. cholerae* in intestinal and fecal samples of aquatic birds [73,87–89]. In the second route, chironomids and copepods, which are known to be reservoirs of *V. cholerae*, attach externally to the feather and feet of birds and facilitate the transport of pathogens [73].

3.2.3. Aquatic-Dissemination Modes

Aquatic plants such as water hyacinth can serve as a dissemination vector of *V. cholerae*. The pathogenic bacteria may concentrate in the plant roots [90,91], which may then be transported by tidal currents across the estuaries from the river mouth to the open sea where the plants may decay due to increased salinity, while the pathogens may survive as they can tolerate moderate salinity and temperature.

Ballast and other non-potable waters from cargo ships are well-established long-distance dispersal mechanisms for human pathogens and waterborne diseases, including cholera. In the early 1990s, an Asian strain of *V. cholerae* transported through ballast water was found to be responsible for a cholera outbreak in Peru [92]. In around the same time period, a Latin American strain of *V. cholerae* was

reported in the ballast water of several ships arriving in the Gulf of Mexico, leading U.S. coast guards to issue an advisory requesting that ballast waters be exchanged in open seas before entry of ships in the U.S. port [20,93]. More recent studies reported the presence of *V. cholerae* in the ballast tanks of ships docked in the ports of Brazil [94] and Singapore [95].

Tiny plastic beads, or “nurdles”, found on beaches and in rivers and seas around the world, could form a novel means of dispersal for potentially pathogenic *Vibrio spp.*, including *V. cholerae*. In coastal and estuarine waters of the North Sea where *V. cholerae* occurrences have been reported [96], up to 75% of nurdles found on bathing beaches were contaminated with *Vibrio spp.* [97]. The hard surface of plastic debris provides an ideal environment for the formation of biofilm to which *Vibrio* bacteria can bind effectively [98]. Furthermore, the slow degradation of synthetic polymers, in comparison to naturally occurring polymers like chitin, may allow transportation and persistence of *V. cholerae* across coastal and marine environments and act as long-distances transportation vectors.

3.3. Role of *Vibrio cholerae* in Biogeochemical Cycling

The bacteria *V. cholerae* are largely discussed as pathogens affecting humans and aquatic organisms. However, being a dominant bacterium in the marine environment, they also play important roles in the pelagic and benthic biogeochemical cycling, especially participation in marine carbon and nutrients cycles [1]. When colonizing particulate matter, *Vibrio* bacteria secrete an array of hydrolytic enzymes to convert high-molecular-weight polymers such as proteins, lipids, carbohydrates, chitin, and laminarin into small-molecular-weight compounds that can be taken up by other pelagic and benthic microorganisms and incorporated into the microbial loop [27].

One of the most abundant carbon sources in the marine environment is chitin. The annual release of chitin associated with the death of chitin-producing organisms may be more than 2.3 million metric tons per year in the whole marine biocycle [99]. The high-molecular-weight chitin polymers are not available to the food web until they are mineralized into low-molecular-weight GlcNac monomers through the action of chitinase enzymes produced by heterotrophic bacteria including *V. cholerae* [1,79,81]. Chitin degradation is initiated with the adherence of the bacteria to the surface of the particulate matter or organisms with the aid of MSHA pilus [76]. Subsequently, the chitin is degraded in a step-wise process into N-acetyl glucosamine by the concerted action of chitinase and β -N-acetylglucosaminidase [83].

3.4. Climatological Conditions

In coastal and lacustrine regions, the predominant climate-related drivers affecting the distribution of *V. cholerae* and disease transmission rates include water temperature, precipitation, freshwater runoff, drought, sea-level rise, flooding, and storm surge, which in turn influence salinity, turbidity, and plankton abundance and composition [100,101]. Changes in climate forcing and environmental conditions may affect the distribution of *V. cholerae* and disease transmission rates at different timescales (short-term, seasonal, inter-annual, and long-term variations) and over different geographic areas (local, regional, and global). For instance, in Bangladesh, the timing of the monsoon has been shown to influence the seasonal dynamics in *V. cholerae* pathogens, resulting in disease transmission rates remaining low during the summer rains and dry winter, and peaking in spring and autumn [102].

Large-scale patterns of climate variability such as the El Niño Southern Oscillation (ENSO) can alter local and regional temperature and precipitation conditions, which might favor *V. cholerae* growth and increase cholera outbreaks (e.g., [103–107]). For instance, in Bangladesh, short-term variation in cholera transmission rates showed a significant 8–10 month lagged correlation with the global climate index Niño3.4 [102]. In regions under the influence of the monsoon such as in Indian and Bangladesh, positive feedback is observed between an anomalous SST warming in the tropical Pacific following winter El Niño events and the changes in summer monsoon atmospheric circulation that result in enhanced precipitation and river discharge, which may lead to a rise in cholera outbreaks [108,109]. Recently, changes in precipitation patterns associated with El Niño perturbations have also been shown

to impact disease transmission rates in Africa [106]. In addition, through the long-range effects of coupled-ocean-atmosphere teleconnections, El Niño has been suggested as a possible “long-distance corridor” for the oceanic transmission of pathogenic strains of *V. cholerae* between Asia and the Americas [110].

Over long timescales and large geographic areas, the potential impact of climate change on the distribution of cholera has been estimated based on the relationship between *V. cholerae* abundance and the environmental variables of temperature and salinity [54]. Under a moderate climate change scenario, the majority of the coastal areas currently less suitable for *V. cholerae* may become more suitable, including latitudinal expansion in *V. cholerae* range from low to medium and high latitudes and an increment of suitable conditions in open waters. The tight relationship between temperature and *V. cholerae* growth has also been used to forecast the increase and new incidence of pathogenic strains in temperate regions of Northern Europe under the regional warming trend [51,111]. Climate-change-driven sea level rise and changes in precipitation may increase surface extent of water-submerged areas and decrease salinity in coastal regions, which may enhance seasonal and geographical availability of habitat suitable for *V. cholerae*. Ocean acidification associated with increasing CO₂ emissions may reduce attachment rates of *V. cholerae* to zooplankton hosts [80,112]. However, more research is needed in this area as high CO₂ levels have also been shown to enhance the diversity of the particle-attached bacterial community [113], influence the dynamic and diversity of plankton community, and in some instances, has been shown to reduce development of mesozooplankton species including copepods and to alter trophic interactions [114], which in turn could also affect growth and distribution of bacteria such as *V. cholerae*.

4. Surveillance and Forecast of Aquatic Reservoirs of Vibrio and Cholera Disease Outbreaks: Existing Approaches and Development Opportunities

An increasing number of human health and epidemiological studies are using a combination of in-situ and remote-sensing data for monitoring, surveillance, forecast, and risk mapping of pathogen occurrence and disease outbreaks (e.g., [7,115–117]). Although microbial pathogens cannot be sensed directly by satellite sensors, the remotely-sensed data can be used to infer their presence. To date, the majority of modeling approaches are based on empirical relationships between pathogen presence/absence or abundance or disease incidence, and a series of bio-physical covariates, such as salinity, sea surface temperature (SST), sea surface height (SSH), pH, dissolved oxygen concentration, Chlorophyll-a concentration, plankton biomass, land cover type, precipitation, and humidity or vapor pressure (e.g., [5,52,116,118–120]).

4.1. Predictive Models Developed Using Ocean-Color Remote-Sensing Data

Ocean-color sensors measure water-leaving reflectance in spectrally contiguous bands in the spectral range of visible wavelengths of the light emerging from the water surface. The remote-sensing reflectance is then used as the basic input to many derived-product algorithms such as inherent optical properties, diffuse attenuation, particulate matter, and chlorophyll-a. The concentration of chlorophyll-a, the primary photosynthetic pigment found in phytoplankton, varies seasonally following the growth and decline of phytoplankton populations. It is the key variable required to estimate primary production (i.e., the rate at which organic carbon is produced by phytoplankton cells), providing unique information on the dynamics of the marine food chain and the biological carbon cycle. Remotely-sensed chlorophyll-a concentration can be retrieved in marine and fresh-waters, allowing us to monitor phytoplankton distribution at high temporal (<1 day) and spatial (<1 km) resolutions from regional to global scales.

To assess the current status of methods and approaches that use ocean-color observations to survey and forecast *Vibrio spp.* occurrence and/or cholera disease incidence, we conducted a structured literature search using PubMed query tools from January 1950 to August 2019, with the keywords cholera; *Vibrio*; chlorophyll; ocean-color; satellite; and remote-sensing. Additional articles and reports

were searched in reference lists of published articles, and using a Google Scholar query between January 1950 and August 2019. The latter query returned 2460 results. The titles and abstracts of the top 10% of the results sorted by relevance were screened. Combining the results from all searches, a total of 16 studies were found to include satellite ocean-color data in their analysis and/or to use the data as a covariate in the development of predictive models of *Vibrio spp.* or cholera dynamics (Table 1).

Table 1. Studies using ocean-color remote-sensing observations to survey and forecast *Vibrio spp.* occurrence or cholera disease outbreaks. RS = remote sensing.

Predicted variable	Covariate	Method	Study Region and Period	Satellite Sensor or Product	Reference
<i>Vibrio parahaemolyticus</i> densities in oyster meat	RS: SST, Chlorophyll-a Other: salinity	Multilinear regression model	British Columbia, Canada; 2003–2015	Multi-scale Ultra-high-resolution SST Analysis, MODIS	[121]
Cholera incidence	RS: SST, SSH, Chlorophyll-a Other: precipitation, temperature	Macro environment–SIR model and multilinear regression analysis of environmental drivers	Zhejiang province, China; 2001–2008	AVHRR, TOPEX/Poseidon and Jason-1, SeaWiFS	[47]
Cholera incidence	RS: SST, SSH, Chlorophyll-a	Multilinear regression model	China; 1999–2008	AVHRR TOPEX/Poseidon and Jason-1, SeaWiFS	[122]
<i>Vibrio cholerae</i> habitat suitability index	RS: Chlorophyll-a, SST, Photosynthetically Available Radiation Other: salinity, pH, O ₂ , nitrate, phosphate	Ecological niche model	Global oceans; 2005–2010	MODIS aqua, SeaWiFS	[54]
Cholera incidence	RS: Chlorophyll-a, precipitation Other: ENSO and DMI climate indices	Inhomogeneous Markov Chain model	Lake Kivu region, DRC; 2002–2012	MODIS aqua, TRMM	[119]
Cholera incidence	RS: reflectance at 412 and 555 nm	Satellite Water Marker (SWM) model based on RS reflectance	Bay of Bengal, Mozambique Channel; 1998–2009	SeaWiFS	[123]
Cholera incidence	RS: Chlorophyll-a	Correlation analyses	Bay of Bengal coastal and offshore; 1998–2007	SeaWiFS	[124]
Cholera incidence	RS: Chlorophyll-a Other: precipitation, fishing activities	Time-series and correlation analyses	Lake Kivu region, DRC; 2002–2006	MODIS aqua	[125]
Cholera incidence	RS: SST, SSH, Chlorophyll-a Other: socio-economic status	Generalized linear model	Bangladesh, Bay of Bengal; 2003–2007	AVHRR, Jason-1, SeaWiFS	[126]
Cholera incidence	RS: Chlorophyll-a Other: river discharge data	Analysis of annual variations	Bay of Bengal, Mozambique Channel; 1997–2010	SeaWiFS	[6]
Cholera incidence	RS: SST, SSH, (Chlorophyll-a)	Correlation analyses	Bangladesh, Bay of Bengal; 1992–1995 and 1997–1998	AVHRR, TOPEX/Poseidon, (SeaWiFS)	[116]
Cholera incidence	RS: SST, SSH, Chlorophyll-a	Analysis of interannual variations	Bangladesh, Bay of Bengal; 1998–2002	AVHRR, TOPEX/Poseidon, SeaWiFS	Colwell and Calkins, unpub. data reported in [16,127]

Table 1. Cont.

Predicted variable	Covariate	Method	Study Region and Period	Satellite Sensor or Product	Reference
Cholera incidence	RS: SST, Chlorophyll-a, precipitation	Generalized linear model	Bangladesh, Matlab, India, Kolkata, Bay of Bengal; 1998–2006	NOAA Optimally Interpolated product, SeaWiFS, Global Precipitation Climatology Project (GPCP)	[44]
Cholera incidence	RS: SST, SSH, Chlorophyll-a, precipitation	Linear regression analyses	KwaZulu-Natal, South Africa; 2000–2001	AVHRR, Topex/Poseidon, SeaWiFS, Merge of infrared and microwave satellite estimates with rain gauge data (GPCP)	[128]
Cholera incidence	RS: SST, SSH, Chlorophyll-a Other: Precipitation, temperature, river discharge or height	Multivariate regression analyses	Matlab, Bangladesh, Hue, Vietnam; 1997–2003	AVHRR, TOPEX/Poseidon and Jason-1, SeaWiFS	[48]
<i>Vibrio parahaemolyticus</i> densities in oyster meat	RS: SST, turbidity, Chlorophyll-a Other: salinity, bottom water temperature	Regression analyses	Alabama coastal region, USA; 1999–2000	AVHRR, SeaWiFS	[129]

In summary, based on the structured literature search, studies that were found to include ocean-color observations in their analyses have investigated predictive skills of: (a) Chlorophyll-a concentration (either as a single explanatory variable or in combination with other environmental covariates) in relation to cholera cases (12 out of 16 studies, Table 1), (b) *V. cholerae* habitat suitability (one study, [54]), or (c) *V. parahaemolyticus* density in oysters (two studies, [121,129]). Covariates investigated in addition to chlorophyll-a, included remotely-sensed observations of SST, SSH, precipitation, and field measurements of salinity, pH, bottom temperature, phyto- and zoo-plankton biomass, river discharge, climate indices, and socioeconomic status. Furthermore, one study developed a satellite water marker (SWM) model that relates coastal water conditions to seasonal cholera incidence [123]. More details about the methodology, geographical coverage, and predictive skill of the different models reported in Table 1 are presented in Sections 4.1.1–4.1.4.

4.1.1. Ocean-Color and Cholera Cases

In coastal regions, such as the Bay of Bengal in Bangladesh and India (Colwell and Calkins, unpub. data; [6,17,44,116,123,124,126]), Mozambique Channel [6,123], Zhejiang province in China [47,122], KwaZulu-Natal province in South Africa [128], and in the inland Lake Kivu region in the Democratic Republic of the Congo [119,125], chlorophyll-a was found to be a significant explanatory variable, with best results often obtained using time-lag correlation between one and six months. Contrasting results were found in the coastal region of Hue, Vietnam, where chlorophyll-a was not significantly associated with the probability of cholera outbreak. However, this latter finding may be related to infrequent cholera epidemics and lull in cholera cases between outbreaks in the region during the study period 1997–2003.

In the coastal regions of the Bay of Bengal and the Mozambique Channel, an SWM model depicting coastal water conditions, suitable for *V. cholerae* bacteria, was utilized, based on the variability of the difference between remote-sensing reflectance in the blue (412 nm) and green (555 nm) wavelengths, which can be related to seasonal incidence of cholera [123]. The SWM index is bounded between physically separable wavelengths for relatively clear (blue) and turbid (green) water. Using the SWM model, prediction of cholera with reasonable accuracy at least two months in advance can potentially

be achieved in endemic coastal regions in spring in Bangladesh and in winter in Mozambique, respectively [123]. Comparative analysis, reported by [123], showed higher predictive ability for SWM (predicted $r^2 = 78\%$ and 57%) than chlorophyll-a (predicted $r^2 = 58\%$ and 23%) in Bangladesh and Mozambique regions respectively. These results suggest that SWM captures biological properties in coastal waters that may not be represented in chlorophyll algorithms. The correlation between detrended anomalies of October–November–December Chlorophyll-a and a positive SWM index, indicative of suitable habitat for *V. cholerae* is shown in Figure 2c for the period 1997–2017. High positive correlations are observed in coastal regions where the water conditions are more turbid and associated with changes in phytoplankton chlorophyll-a.

4.1.2. Ocean-Color and *V. cholerae* Habitat Distribution

The prediction of most suitable areas for potential *V. cholerae* distribution has been investigated in oceanic and coastal regions across the world on the basis of a mathematical representation of their known distribution in environmental space, or so-called realized ecological niche. This approach, referred to as ecological niche modeling, has been used to assess the influence of 12 environmental covariates, including SST, salinity, pH, dissolved oxygen, nutrient concentrations, photosynthetically available radiation, and chlorophyll-a concentration [54]. The results indicate that chlorophyll-a, pH, SST, and salinity could explain most of the variability, with chlorophyll-a having the highest predictive power (49% relative contribution). These findings are consistent with the key environmental factors identified to trigger cholera outbreaks in studies based on empirical relationships between environmental covariates and cholera incidence (e.g., [6,17,44,116]). In the northern Indian Ocean, contemporary distribution of suitable areas for *V. cholerae* predicted by the ecological niche model [54] is in general agreement with the location of maximum risk of cholera incidence predicted by the SWM model [123], although differences can be seen, especially in coastal regions (Figure 2).

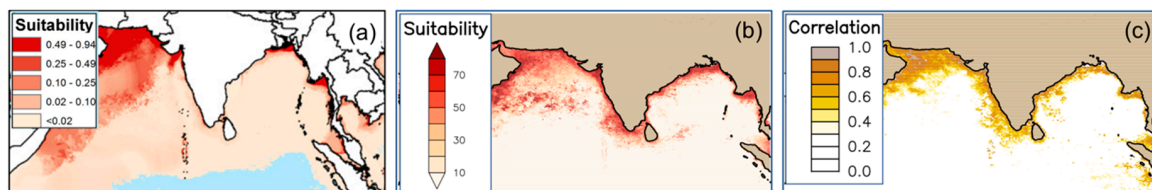


Figure 2. Habitat suitability for *V. cholerae* in the northern Indian Ocean inferred from (a) [54] the ecological niche model (Figure 2a is adapted from [54] their Figure 4) and (b) [123] the satellite water marker (SWM) model applied to the European Space Agency Ocean Color Climate Change Initiative (ESA OC-CCI) remote-sensing reflectance data [130]. The maximum values of SWM (in percent) over the period 1997–2017 are shown. The correlation between chlorophyll-a and satellite water marker is shown in (c). Pearson correlation has been performed using detrended anomalies of October–November–December (OND) chlorophyll-a and OND satellite water marker over the period 1997–2017. OND corresponds to the months analyzed in [123] in the Bengal Delta region. Positive values of SWM, indicating suitable habitat for *V. cholerae* associated with cholera incidence, are used in the correlation analysis. The high positive correlation found in coastal waters suggests a connection between oceanic plankton abundance and cholera incidence in OND. In (c), white color indicates non-significant correlation values. Chlorophyll-a data were obtained from ESA OC-CCI version 4 [130] and satellite water marker data were calculated as indicated in (b).

4.1.3. Ocean-Color and *V. parahaemolyticus* in Oysters

Predictive models of *V. parahaemolyticus* in oysters showed inconstant findings, with a study of British Columbia oysters reporting no association with remote-sensing chlorophyll-a [121], whereas a study of Alabama oysters showed significant relationship with remote-sensing chlorophyll-a after correcting for the effects of temperature and salinity [129].

4.1.4. Local and Regional Specificity

Inconsistent findings regarding the influence of ocean-color and other environmental covariates on *Vibrio* bacteria abundance or cholera cases may be due to differences in spatial (e.g., study area extent, grid size) and temporal (e.g., weekly, monthly, or annual observations, length of data records) data resolution and coverage, differences in the ecological systems (e.g., freshwater, coastal or open ocean waters), differences in the socio-economic context (e.g., sanitation and access to drinking water, raw sea-food consumption), and differences in the disease epidemiological patterns (uni- or bi-annual peaks, outbreaks of primary and secondary cases). Overall, outbreaks of primary cases, resulting from environment-to-human transmission, will be influenced by regional-scale environmental factors, whereas secondary cases, consisting of human-to-human transmission, will primarily depend on local-scale socio-economic factors. Furthermore, outbreaks in coastal systems may have different dominant drivers than in inland systems because they are not only affected by climatic and geographic conditions, but also by oceanic conditions. For instance, cholera incidence data from the coastal Mathbaria region of Bangladesh show endemic patterns with a single peak in the spring while further inland, in other districts of the Ganges-Brahmaputra-Meghna basin (Dhaka, Matlab, Bakerganj, and Kolkata) bi-annual peaks pattern is observed with outbreaks in the spring and post-monsoon in the fall [6,43,44,131,132]. In most affected areas of coastal Mozambique, infection patterns are characterized by a single annual peak in the spring [6]. On the other hand, in landlocked regions such as the East African lake region, intra-annual patterns of cholera vary according to the location, and peaks are generally observed during post-flood situations or after extreme precipitation events [119,125].

4.2. Surveillance and Forecast of *V. cholerae* Reservoirs and Cholera Disease Outbreaks: Development Opportunities from Ocean-Color Remote-Sensing

4.2.1. Sensor-Related Developments

Over the past three decades, national and international space agencies such as the US National Aeronautics and Space Administration (NASA), European Space Agency (ESA), the European Organisation for the Exploitation of Meteorological Satellites (EUMETSAT), The China National Space Administration and State of (CNSA), the Indian Space Research Organisation (ISRO), the Japan Aerospace Exploration Agency (JAXA), the Korean Space Agency, and the French National Centre for Space Studies (CNES) have deployed and operated a range of ocean-color sensors dedicated to measure water-leaving radiance in the visible part of the spectrum [133]. A review of the current status and future perspective of ocean-color observations presented in [134] shows that the sensors deployed have different swath width, spectral coverage, number of wavelength bands (8 to 21), spatial resolution (~300 m to 4 km), temporal frequency (from <1 h to ~4 days), orbit (polar or geostationary), and operate over different time spans (from few months to > decade). The range of characteristics of these sensors are bound by technological and scientific advances, and have been developed to meet user requirements for different applications. For instance, sensors with: high-spatial resolution (~300 m) are particularly suited to study sub-mesoscale processes; high-temporal frequency (<1 day) allows us to study diurnal processes; large number of wavebands permits development of retrieval algorithms for various water constituents and their refinement in complex coastal waters. For the purpose of climate studies, the Global Climate Observing System (GCOS) has identified the requirements for the essential climate variables of remote-sensing reflectance and chlorophyll-a, in terms of data frequency (daily and weekly), spatial resolution (4 km), uncertainty (5% and 30% respectively), and stability (0.5% and 3% respectively) [134]. However, the differences in sensor characteristics make the process of sensor calibration inter-comparison and validation particularly challenging. To address these issues, the ESA Ocean-Colour Climate Change Initiative (OC-CCI) program was launched in 2011, to develop and validate algorithms to meet requirements for consistent, stable, error-characterized merged ocean-color data from multi-sensor archives, including SeaWiFS, Aqua-MODIS, MERIS, and VIIRS. The merged

products provide the longest continuous record (more than two decades) of ocean-color observations with global coverage at 1 to 4 km and daily resolution [130].

In addition to the OC-CCI data archive, observations at high-spatial resolution (~300 m) are becoming increasingly available, with the launch since 2016 of a series of Sentinel missions with sensors dedicated to measure ocean color, SST, and surface topography variables (please see review about relevance and applications of other remote-sensing data in Section 5). Ocean-color sensors onboard the Sentinel-3 missions are presently used and validated to retrieve data on phytoplankton and other water constituents, and are currently being evaluated for their incorporation into the OC-CCI time series [130]. Sentinel-3 Ocean and Land Colour Instrument (OLCI), which is operated by EUMETSAT, provide significant improvements when compared to previous ocean-color sensors, including an increase in the number of spectral bands (from 15 in MERIS to 21 in OLCI), sun-glint mitigation, improved coverage of the global ocean (<2 days with two satellites in constellation, where MERIS is ~15 days), complete overlap with other sensors such as the Sea and Land Surface Temperature Radiometer (SLSTR), which allows us to analyze ocean-color and SST observations in synergy [135]. As part of the space component of the Copernicus program, Sentinel-3 has moved ocean color into the operational domain for the coming decade, with two platforms currently in orbit (Sentinel-3A and Sentinel-3B) and at least two further planned (3C and 3D). Furthermore, data archives of land-designed sensors such as Landsat-8 and Sentinel-2 have also been explored to develop algorithms to retrieve information on phytoplankton and particulate matter. The land sensors have the advantage to provide data at very-high spatial resolution (~30 m), which is most relevant for investigating the dynamics of water constituent at local scale, such as in coastal areas and lakes.

Other remote-sensing platforms, which can carry small-size and lightweight sensors that can measure water-leaving radiance a few meters above the water, include airplanes and unmanned aerial vehicles (UAV) such as balloons or drones [136]. The advantages of these platforms over satellites are further improvement in spatial resolution and the potential to avoid disturbances of the optical signal due to cloud coverage. Furthermore, hyperspectral technology developments have resulted in UAV-compatible smaller and lighter sensors, which are characterized by narrow contiguous spectral bands over a continuous spectral range. Hyperspectral measurements in the spectral range of visible wavelengths are being investigated to produce novel retrieval algorithms for water constituents such as Chlorophyll-a, turbidity, and total suspended solids, providing new perspective for water quality monitoring in shallow coastal and inland waters [137,138].

To date, a limited number of studies (~16) have reported using ocean-color remote sensing to develop applications related to *Vibrio* bacteria habitat suitability and/or cholera disease incidence (Table 1). The data sources, types, spatio-temporal resolution, and the predictive models used, as well as their applications varied from region to region, and were shown to depend on the epidemiological data (e.g., weekly to annual report of bacteria abundance or cholera cases at local, district, or state level). To produce comprehensive recommendation of the requirements for ocean-color remote-sensing data in the context of the *Vibrio* pathogen or cholera applications will require user-engagement review amongst research communities, such as epidemiologists, clinicians, modelers, remote sensing, climate, and social researchers, as well as consultation of stakeholders and end-users, including coastal or lake-shore populations, fishermen, boat-tourism industry workers, port officers, environmental regulators, NGOs, decision-makers, and health service officials. This would be very useful to do in the future, however is beyond the scope of the present paper.

4.2.2. Applications-Related Development

Since the launch of the Coastal Zone Color Scanner (CZCS) by NASA in 1978, ocean-color products have continuously been developed and validated, and transitioned to scientific applications such as in research on the carbon and nitrogen cycles, biogenic trace gases, and in operational mode for fisheries management, harvesting, aquaculture, water quality assessment, harmful algal blooms (HABs) detection, tracking, and prediction. Some of the products developed for these applications may also be relevant to

study the geographic distribution and temporal dynamics of the aquatic reservoirs of *V. cholerae* and help us to better characterize the ecological and biogeochemical signatures of the bacteria.

Based on the environmental interactions of *V. cholerae* described in Section 3, we have reviewed existing ocean-color products that may be used to monitor and forecast aquatic reservoirs of *V. cholerae*, and possible transmission routes of the disease (Table 2).

Table 2. Existing ocean-color products with realized or potentially-new applications on environmental reservoirs of *V. cholerae*.

Application	Status	Environmental Interaction	Reservoir	Ocean-Color Product	Ocean-Color Product Reference
Reservoir distribution and cholera outbreaks	Realized (references in Table 1)	Host–pathogen	Phytoplankton biomass	Total chlorophyll-a	[139–141]
Reservoir distribution and cholera outbreaks	Realized Jutla et al., 2013	Host–pathogen	Phytoplankton biomass and suspended matter	Satellite Water Marker based on Rrs	[123]
Reservoir distribution	Potential	Host–pathogen	Phytoplankton size structure	Micro-, nano-, picohytoplankton chlorophyll-a	[142–145]
Reservoir distribution	Potential	Host–pathogen	Phytoplankton functional groups	Diatoms, Coccolithophores, Phaeocystis, Prochlorococcus, Synechococcus, Nano-Eukaryotes	[146–149]
Reservoir distribution	Potential	Host–pathogen	Chitin-containing phytoplankton	Diatoms	[150]
Reservoir temporal dynamics	Potential	Host–pathogen	Phytoplankton phenology	Timings of initiation, peak, termination, and duration	[151–155]
Biogeochemical cycles regulation	Potential	Carbon cycle	Phytoplankton organic carbon productivity	Primary production	[156]
Biogeochemical cycles regulation	Potential	Carbon cycle	Phytoplankton carbon	Total phytoplankton carbon	[157–160]
Biogeochemical cycles regulation	Potential	Carbon cycle	Phytoplankton carbon	Micro-, nano-, picohytoplankton carbon	[159,160]
Reservoir distribution	Potential	Host–pathogen	Suspended matter	Turbidity, total suspended matter	[161]
Biogeochemical cycles regulation	Potential	Nutrients, Carbon cycle	Particulate organic matter	Particulate organic carbon	[162,163]
Biogeochemical cycles regulation	Potential	Carbon cycle	Particulate inorganic matter	Particulate inorganic carbon	[164,165]
Biogeochemical cycles regulation	Potential	Carbon cycle	Carbon export, acidification	Coccolithophores	[166,167]
Biogeochemical cycles regulation	Potential	Nutrients, Carbon cycle	Dissolved organic matter	Colored dissolved organic matter	[168–170]

5. Applications of Satellite Remote-Sensing to Cholera Epidemics: Supporting Sustainable Development Goals and Targets

Satellite remote-sensing observations, such as ocean-color, SST, SSH, and precipitation, have supplied mechanistic insights that support the construction of predictive models of both *V. cholerae*

habitat distribution and cholera disease outbreaks. In particular, the studies reviewed in Table 1 have highlighted the importance of including covariates of terrestrial nutrient influx and abundance of planktonic hosts, which are key environmental processes in freshwater and coastal regions of cholera endemic countries. Figure 3 shows possible ocean corridors for cholera outbreaks in coastal tropical regions based on 20 years of ESA OC-CCI ocean-color data.

Ocean-color provides information on phytoplankton abundance and is related to the increased presence of zooplankton. The *V. cholerae* bacteria may attach themselves to the phyto- and zoo-plankton, and particularly to diatoms and copepods containing chitin, which has been reported as an effective chemotactic attractant and may help in the formation of biofilms (see Section 3.2). The plankton hosts may then provide shelter and protection for the *Vibrio* bacteria and support its survival, growth, and dissemination in the aquatic environment. SST and salinity are indicative of growth conditions, with the bacteria growing preferentially in warm ($>15\text{ }^{\circ}\text{C}$), low salinity ($<25\text{ ppt NaCl}$) seawaters [51], as well as the conditions favorable for plankton blooms, which also depend on warm ocean temperatures [171]. SSH relates to human–*Vibrio* contact through tidal intrusion of coastal waters carrying plankton laden with *Vibrio* in inland river systems. Finally, precipitation is also important driver, indicative of intense rainfall events associated with increased river flows, which can minimize tidal intrusion of contaminated coastal waters into inland waters. Incorporating this cartographic information in epidemiological models generates new knowledge of the dynamic of cholera epidemics, with the potential to improve our capability to forecast outbreaks in affected countries, and in turn, reduces risks of waterborne diseases for human health.

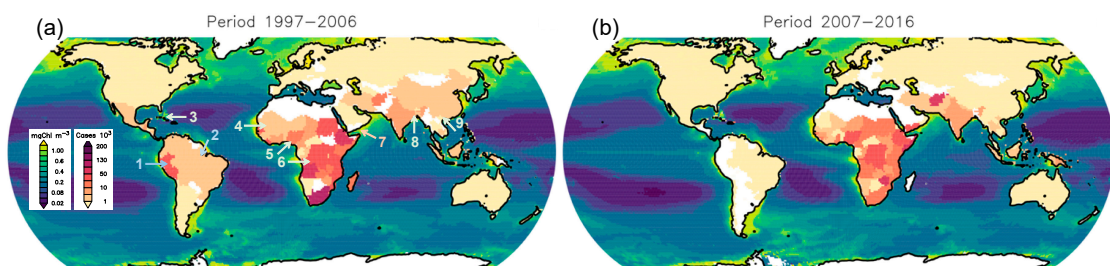


Figure 3. Global map of annual mean chlorophyll-a concentration (ocean) and maximum number of World Health Organization (WHO) reported annual cholera cases (land) over the decades (a) 1997–2006 and (b) 2007–2016. Possible ocean corridors for cholera outbreaks are shown in tropical coastal regions between 30°S to 30°N using numbered arrows. Ocean corridors are defined as locations where plankton intrusion may be possible to inland waters and annual cholera cases have been reported during one or both time periods. The location of possible ocean corridors has been adapted based on [6]. At locations 1 and 2, cholera outbreaks are sporadic. At locations 3 to 9, cholera is endemic (based on definition by [172]). The Amazon River in region 2 is the largest river worldwide by discharge volume of water and by the area of land that drains into it. However, cholera is not reported as endemic in that region, which may be explained by annually constant and high outflows of freshwater that is carried to the sea, and by low population density in the Amazon river basin. At locations 1 and 7, there are no major river inflows into the land and the possible cause of disease outbreaks may be contaminated food or water by *Vibrio* pathogens transported through long-distance oceanic corridors [110] or human travelers [25]. Chlorophyll-a concentration data were obtained from the ESA OC-CCI version 4 [130]. Reported cholera cases were obtained from, and are limited to, the WHO Global Health Observatory data archive. Arrows indicating the location of possible ocean corridors, as well as the color scales for Chlorophyll-a concentration and number of reported cholera cases apply to (a,b). White color means that no data were available.

To assess the potential of satellite applications to support the achievement of Sustainable Development Goals, we have reviewed the knowledge gaps and research priorities on water-borne diseases which have been identified in the 10 year synthesis report ‘Global Goals Mapping: the Environment Human Landscape’ [173]. We found that applications of satellite remote-sensing

to cholera epidemics may help to address some of the knowledge gaps for SDG targets on 3-Health, 6-Water quality, 13-Climate, and 14-Life under the water. We have mapped, for each relevant SDG target, the research priorities on water-borne diseases that can be advanced using remote-sensing. We indicate how these possible advancements might transit to societal benefits, and list SDG indicators that might be used to evaluate impact (Table 3).

Table 3. Potential of satellite applications to address knowledge gaps on water-borne diseases and support achievement of Sustainable Development Goals (SDGs) targets on 3-Health, 6-Water quality, 13-Climate, and 14-Life under the water. For each target and indicator, the reference number in square brackets is based on the numbering presented in the SDGs 2030 agenda.

Goal	Target	Support from Satellite Applications	Indicator of Impact
3-Health	[3.3] Combat epidemics of water-borne diseases; [3.d] Strengthen capacity for early warning, risk reduction and management of national and global health risks	<ul style="list-style-type: none"> - Improve knowledge on the transmission patterns of the <i>Vibrio cholerae</i> pathogens in affected countries → the information will be useful for health services to help provide the most adapted and efficient treatment for the affected local populations, and to increase chances of recovery; - Improve surveillance systems and strengthen the capacity of affected countries to produce early warning and risk maps for cholera outbreaks → the improved/local/regional forecast systems may be delivered to national agencies for operational use and the risk warning may be placed in the public domain to reduce public health risks. 	[3.3.5] a reduction in the number of people requiring treatment against <i>Vibrio</i> disease; [3.9.2] a reduction in mortality rate associated with exposure to contaminated water; [3.d.1] an increase in capacity for disaster mitigation in affected areas.
6-Water quality	[6.3] Improve water quality by reducing pollution, halving the proportion of untreated wastewater; [6.5] Implement integrated water resource management	<ul style="list-style-type: none"> - Provide evidence on <i>Vibrio</i> disease hotspots → this information will help government authorities to identify areas where microbial and antibiotic pollution should be treated as a priority. - Improve knowledge of the transmission routes and dynamics of cholera pathogens in the lacustrine and coastal ecosystems in relation to climate variability and disease outbreaks → this information will support increased preparedness along the transmission routes, and integration of locally-targeted water sanitation control measures that will help to interrupt the transmission routes. 	[6.b.1] an increase in the number of actions taken by local administrations to treat sources of pollution, and to engage the local communities in water and sanitation management.
13-Climate	[13.1] Strengthen resilience and adaptive capacity to climate-related hazards and natural disasters	<ul style="list-style-type: none"> - Improve knowledge of the influence of extreme weather events and climate variability on the incidence of cholera outbreaks and the contamination routes of <i>Vibrio</i> pathogens → this will help to prioritize policy measures for health service preparedness and population awareness when high-risk climate events occur, and hence improve cholera-disaster risk mitigation. 	[13.3.1] an increase in the number of countries that recognize the need to integrate climate-related risk in their early warning systems for cholera outbreaks, and in their adaptation and mitigation plans (to reduce impact and risk of cholera outbreaks).
14-Marine Life	[14.1] Prevent and significantly reduce marine pollution of all kinds; [14.2] Sustainably manage and protect marine and coastal ecosystems to avoid significant adverse impacts and achieve healthy and productive oceans	<ul style="list-style-type: none"> - Provide evidence on the extent to which lacustrine and coastal communities are suffering from <i>Vibrio</i> diseases → this information can be used to support the development of sustainable management plans. 	[14.c.1] an increase in the number of countries that incorporate ecosystem-based management in their stewardship of coastal ecosystems and their resources.

The potential of remote sensing to provide support to the implementation of SDGs may be achieved only if technology transfer is effectively carried out to affected nations. Based on an analysis of situations in the Bengal Delta Region (Bangladesh) and in the Vembanad Lake region in Kerala state in India, [120] have provided recommendations on how to transfer and make best use of remote-sensing technology to build resilience against water-borne disease outbreaks. Primary factors to achieve these include education of all social classes, as well as credibility and timeliness of scientific advice provided as preventive measures and during emergencies. In addition, the engagement of citizens in the collection of scientific observations—related to social (e.g., sanitation, access to drinking water, infrastructure damage during floods) and environmental (e.g., water temperature, color, clarity, [174]) conditions can be particularly useful for the development and validation of predictive models of *Vibrio* bacteria growth and risks of disease outbreaks. Furthermore, the use of smartphone applications to record and disseminate citizen observations has proven to be critical to providing timely updates on risk of outbreaks and/or spread of the disease [175,176].

6. Conclusions

Ocean-color remote sensing observations are increasingly used to map and forecast cholera disease outbreaks and the distribution of *V. cholerae* environmental reservoirs in fresh, coastal, and open-ocean systems. The ocean-color data have been found to relate to the increase in phytoplankton that can be associated with increase in zooplankton, which forms key environmental reservoirs of *V. cholerae*, and reflect the intrusion of coastal waters carrying plankton laden with *V. cholerae* into inland waters. Human infection may then be caused by drinking water and/or consuming seafood contaminated with pathogenic *V. cholerae* bacteria.

In predictive model of *V. cholerae* bacteria distribution and primary disease transmission, ocean-color is often reported as a major explanatory variable, and the models are performing best when ocean-color is used in combination with other remotely-sensed variables such as SST, SSH, precipitation, and in-situ measurements, including salinity, pH, bottom temperature, phyto- and zoo-plankton biomass, river discharge, and climate indices. Secondary disease transmission is strongly dependent on access to drinking water and sanitation, and consumption of seafood, which are best reflected by including data on the socio-economic status of the populations.

From the wide range of models that have been developed for cholera outbreaks (Table 1), and for other infectious diseases [7,18], the level of refinement in time and space mapping and forecast of environmental reservoirs and disease occurrence appears to be related principally to: (a) The understanding of the pathogens' ecology, including its life cycle, interaction with environmental hosts, and transmission routes; (b) the coverage, spatial-temporal resolution, length of time-series data available for mapping, and predictive model developments; and (c) the extent of the mechanistic understanding and previous mapping efforts of disease outbreak dynamics. Refinements of predictive models are anticipated to take place with advancements in satellite sensors, including the availability of multi-decadal merged products, high-resolution and multi-spectral observations, as well as in development of satellite applications, which have the potential transit to societal benefits. These advancements will help to further actions towards sustainable human–environment interactions, for instance, by providing policy information on coastal areas where microbial and antibiotic pollution should be treated as priorities, and on country-level preparation needs of cholera vaccine stockpile [177]. In turn, these water management actions will also help to regulate the threat of waterborne diseases and to meet the needs to reduce the risks of waterborne diseases for human health.

Author Contributions: Conceptualization, M.-F.R., A.A., S.S.; formal analysis, M.-F.R.; investigation, M.-F.R.; data curation, K.M., B.L.; writing—original draft preparation, M.-F.R., M.P., V.V., A.A., S.S., B.L., J.C, K.M., N.M., G.G., T.P.; writing—review and editing, M.-F.R., S.S., A.A., B.L., T.P.; visualization, M.-F.R.; funding acquisition, M.-F.R., S.S., A.A., T.P., G.G., N.M.

Funding: This research was funded by the India–UK water quality research program under the Department of Science and Technology (DST) and the Natural Environment Research Council (NERC) REVIVAL project grant

numbers [NE/R003521/1 and DST/TM/INDO-UK/2k17/64(C)]; the DST—Science and Engineering Research Board under Jawaharlal Nehru Science Fellowship (DST-SERB JNSF) to Trevor Platt, held at the Central Marine Fisheries Research Institute; and the United Kingdom Research and Innovation (UKRI) Towards a Sustainable Earth (TaSE) program under the Japan Science and Technology Agency (JST), the India Department for Biotechnology (DBT) and the NERC project PODCAST grant numbers [NE/S012567/1 and BT/IN/TaSE/71/AA/2018-19].

Acknowledgments: The financial support from DST Government of India and NERC under Indo–UK water call program; and from JST-Japan, DBT-India and UKRI NERC under Towards a Sustainable Earth (TaSE) Japan–India–UK program are acknowledged. The authors are thankful to the directors of CSIR-National Institute of Oceanography and ICAR-Central Marine Fisheries Research Institute for the support and encouragement to complete the work. This work is a contribution to the UKRI-NERC Pathways Of Dispersal for Cholera And Solution Tools (PODCAST) project, the NERC rehabilitation of Vibrio Infested waters of Vembanad Lake: pollution and solution (REVIVAL) project, the NERC National Centre for Earth Observation (NCEO), the European Space Agency Ocean Color Climate Change Initiative (ESA OC-CCI), and to the GEO Blue Planet Water-associated Diseases Working Group supported by a grant from the Partnership for Observation of the Global Ocean (POGO). The authors thank the ESA OC-CCI team for providing chlorophyll data and the World Health Organization (WHO) for providing cholera cases data. The authors further acknowledge Jon White (PML) for technical support with Adobe Reader for Figure 1.

Conflicts of Interest: The authors declare no conflict of interest.

References

- Zhang, X.; Lin, H.; Wang, X.; Austin, B. Significance of *Vibrio* species in the marine organic carbon cycle—A review. *Sci. China Earth Sci.* **2018**, *61*, 1357–1368. [[CrossRef](#)]
- Huq, A.; Haley, B.J.; Taviani, E.; Chen, A.; Hasan, N.A.; Colwell, R.R. Detection, isolation, and identification of *Vibrio cholerae* from the environment. *Curr. Protoc. Microbiol.* **2012**, *26*, 6A-5. [[CrossRef](#)] [[PubMed](#)]
- Chapman, C.; Henry, M.; Bishop-Lilly, K.A.; Awosika, J.; Briska, A.; Ptashkin, R.N.; Wagner, T.; Rajanna, C.; Tsang, H.; Johnson, S.L.; et al. Scanning the Landscape of Genome Architecture of Non-O1 and Non-O139 *Vibrio cholerae* by Whole Genome Mapping Reveals Extensive Population Genetic Diversity. *PLoS ONE* **2015**, *10*, e0120311. [[CrossRef](#)] [[PubMed](#)]
- World Health Organisation; United Nations Children’s Fund. *Wash in the 2030 Agenda: New Global Indicators for Drinking Water, Sanitation and Hygiene*; World Health Organisation: Geneva, Switzerland, 2017; p. 8.
- Colwell, R.R. Global Climate and Infectious Disease: The Cholera Paradigm*. *Science* **1996**, *274*, 2025–2031. [[CrossRef](#)]
- Jutla, A.S.; Akanda, A.S.; Islam, S. Tracking Cholera in Coastal Regions Using Satellite Observations. *JAWRA J. Am. Water Resour. Assoc.* **2010**, *46*, 651–662. [[CrossRef](#)]
- Hay, S.I.; Battle, K.E.; Pigott, D.M.; Smith, D.L.; Moyes, C.L.; Bhatt, S.; Brownstein, J.S.; Collier, N.; Myers, M.F.; George, D.B.; et al. Global mapping of infectious disease. *Philos. Trans. R. Soc. B Biol. Sci.* **2013**, *368*, 20120250. [[CrossRef](#)]
- Andries, A.; Morse, S.; Murphy, R.; Lynch, J.; Woolliams, E.; Fonweban, J. Translation of Earth observation data into sustainable development indicators: An analytical framework. *Sustain. Dev.* **2019**, *27*, 366–376. [[CrossRef](#)]
- Andries, A.; Morse, S.; Murphy, R.J.; Lynch, J.; Woolliams, E.R. Seeing Sustainability from Space: Using Earth Observation Data to Populate the UN Sustainable Development Goal Indicators. *Sustainability* **2019**, *11*, 5062. [[CrossRef](#)]
- Nilsson, M.; Griggs, D.; Visbeck, M. Policy: Map the interactions between Sustainable Development Goals. *Nat. News* **2016**, *534*, 320. [[CrossRef](#)]
- Kitaoka, M.; Miyata, S.T.; Unterweger, D.; Pukatzki, S. Antibiotic resistance mechanisms of *Vibrio cholerae*. *J. Med. Microbiol.* **2011**, *60*, 397–407. [[CrossRef](#)]
- Almagro-Moreno, S.; Pruss, K.; Taylor, R.K. Intestinal Colonization Dynamics of *Vibrio cholerae*. *PLoS Pathog.* **2015**, *11*, e1004787. [[CrossRef](#)] [[PubMed](#)]
- Childers, B.M.; Klose, K.E. Regulation of virulence in *Vibrio cholerae*: The ToxR regulon. *Future Med.* **2007**, *2*, 335–344.
- Cottingham, K.L.; Chiavelli, D.A.; Taylor, R.K. Environmental microbe and human pathogen: The ecology and microbiology of *Vibrio cholerae*. *Front. Ecol. Environ.* **2003**, *1*, 80–86. [[CrossRef](#)]
- Lutz, C.; Erken, M.; Noorian, P.; Sun, S.; McDougald, D. Environmental reservoirs and mechanisms of persistence of *Vibrio cholerae*. *Front. Microbiol.* **2013**, *4*, 375. [[CrossRef](#)] [[PubMed](#)]

16. Grimes, D.J.; Ford, T.E.; Colwell, R.R.; Baker-Austin, C.; Martinez-Urtaza, J.; Subramaniam, A.; Capone, D.G. Viewing Marine Bacteria, Their Activity and Response to Environmental Drivers from Orbit: Satellite Remote Sensing of Bacteria. *Microb. Ecol.* **2014**, *67*, 489–500. [[CrossRef](#)]
17. Jutla, A.S.; Akanda, A.S.; Islam, S. A framework for predicting endemic cholera using satellite derived environmental determinants. *Environ. Model. Softw.* **2013**, *47*, 148–158. [[CrossRef](#)]
18. Semenza, J.C.; Trinanes, J.; Lohr, W.; Sudre, B.; Löfdahl, M.; Martinez-Urtaza, J.; Nichols, G.L.; Rocklöv, J. Environmental Suitability of Vibrio Infections in a Warming Climate: An Early Warning System. *Environ. Health Perspect.* **2017**, *125*, 107004. [[CrossRef](#)]
19. Colwell, R.; Huq, A. Marine ecosystems and cholera. *Hydrobiologia* **2001**, *460*, 141–145. [[CrossRef](#)]
20. Lipp, E.K.; Rose, J.B. The role of seafood in foodborne diseases in the United States of America. *Rev. Sci. Tech. Off. Int. Epizoot.* **1997**, *16*, 620–640. [[CrossRef](#)]
21. Feldhusen, F. The role of seafood in bacterial foodborne diseases. *Microbes Infect.* **2000**, *2*, 1651–1660. [[CrossRef](#)]
22. Iwamoto, M.; Ayers, T.; Mahon, B.E.; Swerdlow, D.L. Epidemiology of Seafood-Associated Infections in the United States. *Clin. Microbiol. Rev.* **2010**, *23*, 399–411. [[CrossRef](#)] [[PubMed](#)]
23. Barange, M. *Impacts of Climate Change on Fisheries and Aquaculture: Synthesis of Current Knowledge, Adaptation and Mitigation Options*; Food and Agriculture Organization: Rome, Italy, 2018.
24. Mutreja, A.; Kim, D.W.; Thomson, N.R.; Connor, T.R.; Lee, J.H.; Kariuki, S.; Croucher, N.J.; Choi, S.Y.; Harris, S.R.; Lebens, M.; et al. Evidence for several waves of global transmission in the seventh cholera pandemic. *Nature* **2011**, *477*, 462–465. [[CrossRef](#)] [[PubMed](#)]
25. Domman, D.; Quilici, M.L.; Dorman, M.J.; Njamkepo, E.; Mutreja, A.; Mather, A.E.; Delgado, G.; Morales-Espinosa, R.; Grimont, P.A.; Lizárraga-Partida, M.L. Integrated view of Vibrio cholerae in the Americas. *Science* **2017**, *358*, 789–793. [[CrossRef](#)] [[PubMed](#)]
26. Ramamurthy, T.; Mutreja, A.; Weill, F.X.; Das, B.; Ghosh, A.; Nair, G.B. Revisiting the Global Epidemiology of Cholera in Conjunction with the Genomics of Vibrio cholerae. *Front. Public Health* **2019**, *7*, 203. [[CrossRef](#)] [[PubMed](#)]
27. Thompson, J.R.; Polz, M.F. Dynamics of Vibrio Populations and Their Role in Environmental Nutrient Cycling. *Biol. Vibrios* **2006**, 190–203. [[CrossRef](#)]
28. Böer, S.I.; Heinemeyer, E.A.; Luden, K.; Erler, R.; Gerdt, G.; Janssen, F.; Brennholt, N. Temporal and Spatial Distribution Patterns of Potentially Pathogenic Vibrio spp. at Recreational Beaches of the German North Sea. *Microb. Ecol.* **2013**, *65*, 1052–1067. [[CrossRef](#)]
29. Bresnan, E.; Baker-Austin, C.; Campos, C.J.A.; Davidson, K.; Edwards, M.; Hall, A.; Lees, D.; McKinney, A.; Milligan, S.; Silke, J. Human health. *MCCIP Sci. Rev.* **2017**, *2017*, 100–107.
30. Schwartz, K.; Hammerl, J.A.; Göllner, C.; Strauch, E. Environmental and Clinical Strains of Vibrio cholerae Non-O1, Non-O139 From Germany Possess Similar Virulence Gene Profiles. *Front. Microbiol.* **2019**, *10*, 733. [[CrossRef](#)]
31. Binsztein, N.; Costagliola, M.C.; Pichel, M.; Jurquiza, V.; Ramírez, F.C.; Akselman, R.; Vacchino, M.; Huq, A.; Colwell, R. Viable but Nonculturable Vibrio cholerae O1 in the Aquatic Environment of Argentina. *Appl. Environ. Microbiol.* **2004**, *70*, 7481–7486. [[CrossRef](#)]
32. Martinelli Filho, J.E.; Lopes, R.M.; Rivera, I.N.G.; Colwell, R.R. Vibrio cholerae O1 detection in estuarine and coastal zooplankton. *J. Plankton Res.* **2011**, *33*, 51–62. [[CrossRef](#)]
33. Azarian, T.; Ali, A.; Johnson, J.A.; Jubair, M.; Cella, E.; Ciccozzi, M.; Nolan, D.J.; Farmerie, W.; Rashid, M.H.; Sinha-Ray, S.; et al. Non-toxigenic environmental Vibrio cholerae O1 strain from Haiti provides evidence of pre-pandemic cholera in Hispaniola. *Sci. Rep.* **2016**, *6*, 36115. [[CrossRef](#)] [[PubMed](#)]
34. Chávez, M.D.; Sedas, V.P.; Borunda, E.O.; Reynoso, F.L. Influence of water temperature and salinity on seasonal occurrences of Vibrio cholerae and enteric bacteria in oyster-producing areas of Veracruz, México. *Mar. Pollut. Bull.* **2005**, *50*, 1641–1648. [[CrossRef](#)] [[PubMed](#)]
35. Lipp, E.K.; Rivera, I.N.G.; Gil, A.I.; Espeland, E.M.; Choopun, N.; Louis, V.R.; Russek-Cohen, E.; Huq, A.; Colwell, R.R. Direct Detection of Vibrio cholerae and ctxA in Peruvian Coastal Water and Plankton by PCR. *Appl. Environ. Microbiol.* **2003**, *69*, 3676–3680. [[CrossRef](#)] [[PubMed](#)]
36. Gil, A.I.; Louis, V.R.; Rivera, I.N.G.; Lipp, E.; Huq, A.; Lanata, C.F.; Taylor, D.N.; Russek-Cohen, E.; Choopun, N.; Sack, R.B.; et al. Occurrence and distribution of Vibrio cholerae in the coastal environment of Peru. *Environ. Microbiol.* **2004**, *6*, 699–706. [[CrossRef](#)]

37. Graü, C.; Barbera, A.L.; Zerpa, A. Isolation of *Vibrio* spp. And Evaluation of the Sanitary Condition of Bivalve Mollusks *Arca zebra* and *Perna perna* Collected on the Northeastern Coast of Sucre State, Venezuela. *Rev. Cient.* **2004**, *14*, 513–521.
38. Louis, V.R.; Russek-Cohen, E.; Choopun, N.; Rivera, I.N.G.; Gangle, B.; Jiang, S.C.; Rubin, A.; Patz, J.A.; Huq, A.; Colwell, R.R. Predictability of *Vibrio cholerae* in Chesapeake Bay. *Appl. Environ. Microbiol.* **2003**, *69*, 2773–2785. [[CrossRef](#)]
39. Dobbs, F.C.; Goodrich, A.L.; Thomson, F.K.; Hynes, W. Pandemic Serotypes of *Vibrio cholerae* Isolated from Ships' Ballast Tanks and Coastal Waters: Assessment of Antibiotic Resistance and Virulence Genes (tcpA and ctxA). *Microb. Ecol.* **2013**, *65*, 969–974. [[CrossRef](#)]
40. Kiiru, J.; Mutreja, A.; Mohamed, A.A.; Kimani, R.W.; Mwituria, J.; Sanaya, R.O.; Muyodi, J.; Revathi, G.; Parkhill, J.; Thomson, N.; et al. A Study on the Geophylogeny of Clinical and Environmental *Vibrio cholerae* in Kenya. *PLoS ONE* **2013**, *8*, e74829. [[CrossRef](#)]
41. Du Preez, M.; Van der Merwe, M.R.; Cumbana, A.; Le Roux, W. A survey of *Vibrio cholerae* O1 and O139 in estuarine waters and sediments of Beira, Mozambique. *Water SA* **2010**, *36*. [[CrossRef](#)]
42. Mukhopadhyay, A.K.; Basu, A.; Garg, P.; Bag, P.K.; Ghosh, A.; Bhattacharya, S.K.; Takeda, Y.; Nair, G.B. Molecular Epidemiology of Reemergent *Vibrio cholerae* O139 Bengal in India. *J. Clin. Microbiol.* **1998**, *36*, 2149–2152.
43. Sack, R.B.; Siddique, A.K.; Longini, I.M., Jr.; Nizam, A.; Yunus, M.; Islam, M.S.; Morris, J.G., Jr.; Ali, A.; Huq, A.; Nair, G.B.; et al. A 4-Year Study of the Epidemiology of *Vibrio cholerae* in Four Rural Areas of Bangladesh. *J. Infect. Dis.* **2003**, *187*, 96–101. [[CrossRef](#)] [[PubMed](#)]
44. de Magny, G.C.; Murtugudde, R.; Sapiiano, M.R.P.; Nizam, A.; Brown, C.W.; Busalacchi, A.J.; Yunus, M.; Nair, G.B.; Gil, A.I.; Lanata, C.F.; et al. Environmental signatures associated with cholera epidemics. *Proc. Natl. Acad. Sci. USA* **2008**, *105*, 17676–17681. [[CrossRef](#)] [[PubMed](#)]
45. Batabyal, P.; Mookerjee, S.; Einsporn, M.H.; Lara, R.J.; Palit, A. Environmental drivers on seasonal abundance of riverine-estuarine *V. cholerae* in the Indian Sundarban mangrove. *Ecol. Indic.* **2016**, *69*, 59–65. [[CrossRef](#)]
46. Ali, M.; Gupta, S.S.; Arora, N.; Khasnobis, P.; Venkatesh, S.; Sur, D.; Nair, G.B.; Sack, D.A.; Ganguly, N.K. Identification of burden hotspots and risk factors for cholera in India: An observational study. *PLoS ONE* **2017**, *12*, e0183100. [[CrossRef](#)] [[PubMed](#)]
47. Xu, M.; Cao, C.X.; Wang, D.C.; Kan, B.; Xu, Y.F.; Ni, X.L.; Zhu, Z.C. Environmental factor analysis of cholera in China using remote sensing and geographical information systems. *Epidemiol. Infect.* **2016**, *144*, 940–951. [[CrossRef](#)]
48. Emch, M.; Feldacker, C.; Islam, M.S.; Ali, M. Seasonality of cholera from 1974 to 2005: A review of global patterns. *Int. J. Health Geogr.* **2008**, *7*, 31. [[CrossRef](#)]
49. Vezzulli, L.; Pruzzo, C.; Huq, A.; Colwell, R.R. Environmental reservoirs of *Vibrio cholerae* and their role in cholera: Environmental reservoirs of *V. cholerae*. *Environ. Microbiol. Rep.* **2010**, *2*, 27–33. [[CrossRef](#)]
50. Vezzulli, L.; Grande, C.; Reid, P.C.; Hélaouët, P.; Edwards, M.; Höfle, M.G.; Brettar, I.; Colwell, R.R.; Pruzzo, C. Climate influence on *Vibrio* and associated human diseases during the past half-century in the coastal North Atlantic. *Proc. Natl. Acad. Sci. USA* **2016**, *113*, E5062–E5071. [[CrossRef](#)]
51. Baker-Austin, C.; Trinanes, J.A.; Taylor, N.G.H.; Hartnell, R.; Siitonen, A.; Martinez-Urtaza, J. Emerging *Vibrio* risk at high latitudes in response to ocean warming. *Nat. Clim. Chang.* **2013**, *3*, 73–77. [[CrossRef](#)]
52. Huq, A.; Sack, R.B.; Nizam, A.; Longini, I.M.; Nair, G.B.; Ali, A.; Morris, J.G.; Khan, M.N.H.; Siddique, A.K.; Yunus, M.; et al. Critical Factors Influencing the Occurrence of *Vibrio cholerae* in the Environment of Bangladesh. *Appl. Environ. Microbiol.* **2005**, *71*, 4645–4654. [[CrossRef](#)]
53. Takemura, A.F.; Chien, D.M.; Polz, M.F. Associations and dynamics of Vibrionaceae in the environment, from the genus to the population level. *Front. Microbiol.* **2014**, *5*, 38. [[CrossRef](#)] [[PubMed](#)]
54. Escobar, L.E.; Ryan, S.J.; Stewart-Ibarra, A.M.; Finkelstein, J.L.; King, C.A.; Qiao, H.; Polhemus, M.E. A global map of suitability for coastal *Vibrio cholerae* under current and future climate conditions. *Acta Trop.* **2015**, *149*, 202–211. [[CrossRef](#)]
55. Kopprio, G.A.; Streitenberger, M.E.; Okuno, K.; Baldini, M.; Biancalana, F.; Fricke, A.; Martínez, A.; Neogi, S.B.; Koch, B.P.; Yamasaki, S.; et al. Biogeochemical and hydrological drivers of the dynamics of *Vibrio* species in two Patagonian estuaries. *Sci. Total Environ.* **2017**, *579*, 646–656. [[CrossRef](#)] [[PubMed](#)]

56. Beardsley, C.; Pernthaler, J.; Wosniok, W.; Amann, R. Are Readily Culturable Bacteria in Coastal North Sea Waters Suppressed by Selective Grazing Mortality? *Appl. Environ. Microbiol.* **2003**, *69*, 2624–2630. [[CrossRef](#)] [[PubMed](#)]
57. Worden, A.Z.; Seidel, M.; Smriga, S.; Wick, A.; Malfatti, F.; Bartlett, D.; Azam, F. Trophic regulation of *Vibrio cholerae* in coastal marine waters. *Environ. Microbiol.* **2006**, *8*, 21–29. [[CrossRef](#)]
58. Westrich, J.R.; Ebling, A.M.; Landing, W.M.; Joyner, J.L.; Kemp, K.M.; Griffin, D.W.; Lipp, E.K. Saharan dust nutrients promote *Vibrio* bloom formation in marine surface waters. *Proc. Natl. Acad. Sci. USA* **2016**, *113*, 5964–5969. [[CrossRef](#)]
59. Zhang, R.; Kelly, R.L.; Kauffman, K.M.; Reid, A.K.; Lauderdale, J.M.; Follows, M.J.; John, S.G. Growth of marine *Vibrio* in oligotrophic environments is not stimulated by the addition of inorganic iron. *Earth Planet. Sci. Lett.* **2019**, *516*, 148–155. [[CrossRef](#)]
60. Fernández-Delgado, M.; García-Amado, M.A.; Contreras, M.; Incani, R.N.; Chirinos, H.; Rojas, H.; Suárez, P. SURVIVAL, INDUCTION AND RESUSCITATION OF *Vibrio cholerae* FROM THE VIABLE BUT NON-CULTURABLE STATE IN THE SOUTHERN CARIBBEAN SEA. *Rev. Inst. Med. Trop. São Paulo* **2015**, *57*, 21–26. [[CrossRef](#)]
61. Faruque, S.M.; Mekalanos, J.J. Phage-bacterial interactions in the evolution of toxigenic *Vibrio cholerae*. *Virulence* **2012**, *3*, 556–565. [[CrossRef](#)]
62. Ellison, C.K.; Dalia, T.N.; Vidal Ceballos, A.; Wang, J.C.Y.; Biais, N.; Brun, Y.V.; Dalia, A.B. Retraction of DNA-bound type IV competence pili initiates DNA uptake during natural transformation in *Vibrio cholerae*. *Nat. Microbiol.* **2018**, *3*, 773–780. [[CrossRef](#)]
63. Suzuki, S.; Hoa, P.T.P. Distribution of Quinolones, Sulfonamides, Tetracyclines in Aquatic Environment and Antibiotic Resistance in Indochina. *Front. Microbiol.* **2012**, *3*, 67. [[CrossRef](#)] [[PubMed](#)]
64. Wilhelm, S.W.; Suttle, C.A. Viruses and Nutrient Cycles in the Sea Viruses play critical roles in the structure and function of aquatic food webs. *BioScience* **1999**, *49*, 781–788. [[CrossRef](#)]
65. Abd, H.; Saeed, A.; Weintraub, A.; Nair, G.B.; Sandstrom, G. *Vibrio cholerae* O1 strains are facultative intracellular bacteria, able to survive and multiply symbiotically inside the aquatic free-living amoeba *Acanthamoeba castellanii*: *Vibrio cholerae* in amoebae. *FEMS Microbiol. Ecol.* **2007**, *60*, 33–39. [[CrossRef](#)] [[PubMed](#)]
66. Wei, Y.; Perez, L.J.; Ng, W.L.; Semmelhack, M.F.; Bassler, B.L. Mechanism of *Vibrio cholerae* Autoinducer-1 Biosynthesis. *ACS Chem. Biol.* **2011**, *6*, 356–365. [[CrossRef](#)] [[PubMed](#)]
67. Conner, J.G.; Teschler, J.K.; Jones, C.J.; Yildiz, F.H. Staying alive: *Vibrio cholerae*'s cycle of environmental survival, transmission, and dissemination. *Microbiol. Spectr.* **2016**, *4*. [[CrossRef](#)]
68. Madico, G.; Checkley, W.; Gilman, R.H.; Bravo, N.; Cabrera, L.; Calderon, M.; Ceballos, A. Active surveillance for *Vibrio cholerae* O1 and vibriophages in sewage water as a potential tool to predict cholera outbreaks. *J. Clin. Microbiol.* **1996**, *34*, 2968–2972.
69. Jensen, M.A.; Faruque, S.M.; Mekalanos, J.J.; Levin, B.R. Modeling the role of bacteriophage in the control of cholera outbreaks. *Proc. Natl. Acad. Sci. USA* **2006**, *103*, 4652–4657. [[CrossRef](#)]
70. Hood, M.A.; Winter, P.A. Attachment of *Vibrio cholerae* under various environmental conditions and to selected substrates. *FEMS Microbiol. Ecol.* **1997**, *22*, 215–223. [[CrossRef](#)]
71. Paz, S.; Broza, M. Wind Direction and Its Linkage with *Vibrio cholerae* Dissemination. *Environ. Health Perspect.* **2007**, *115*, 195–200. [[CrossRef](#)]
72. Paz, S. The cholera epidemic in Yemen—How did it start? The role of El Niño conditions followed by regional winds. *Environ. Res.* **2019**, *176*, 108571. [[CrossRef](#)]
73. Halpern, M.; Senderovich, Y.; Izhaki, I. Waterfowl—The Missing Link in Epidemic and Pandemic Cholera Dissemination? *PLoS Pathog.* **2008**, *4*, e1000173. [[CrossRef](#)] [[PubMed](#)]
74. Senderovich, Y.; Izhaki, I.; Halpern, M. Fish as Reservoirs and Vectors of *Vibrio cholerae*. *PLoS ONE* **2010**, *5*, e8607. [[CrossRef](#)] [[PubMed](#)]
75. Halpern, M.; Izhaki, I. Fish as Hosts of *Vibrio cholerae*. *Front. Microbiol.* **2017**, *8*, 282. [[CrossRef](#)] [[PubMed](#)]
76. Frischkorn, K.R.; Stojanovski, A.; Paranjpye, R. *Vibrio parahaemolyticus* type IV pili mediate interactions with diatom-derived chitin and point to an unexplored mechanism of environmental persistence. *Environ. Microbiol.* **2013**, *15*, 1416–1427. [[CrossRef](#)] [[PubMed](#)]
77. Weiss, I.M.; Schönitzer, V.; Eichner, N.; Sumper, M. The chitin synthase involved in marine bivalve mollusk shell formation contains a myosin domain. *FEBS Lett.* **2006**, *580*, 1846–1852. [[CrossRef](#)]

78. Dalusi, L.; Lyimo, T.J.; Lugomela, C.; Hosea, K.M.M.; Sjöling, S. Toxigenic *Vibrio cholerae* identified in estuaries of Tanzania using PCR techniques. *FEMS Microbiol. Lett.* **2015**, *362*, fnv009. [[CrossRef](#)]
79. Meibom, K.L.; Li, X.B.; Nielsen, A.T.; Wu, C.Y.; Roseman, S.; Schoolnik, G.K. The *Vibrio cholerae* chitin utilization program. *Proc. Natl. Acad. Sci. USA* **2004**, *101*, 2524–2529. [[CrossRef](#)]
80. Huq, A.; West, P.A.; Small, E.B.; Huq, M.I.; Colwell, R.R. Influence of water temperature, salinity, and pH on survival and growth of toxigenic *Vibrio cholerae* serovar O1 associated with live copepods in laboratory microcosms. *Appl. Environ. Microbiol.* **1984**, *48*, 420–424.
81. Colwell, R.R. Polyphasic Taxonomy of the Genus *Vibrio*: Numerical Taxonomy of *Vibrio cholerae*, *Vibrio parahaemolyticus*, and Related *Vibrio* Species. *J. Bacteriol.* **1970**, *104*, 410–433.
82. Li, X.; Wang, L.X.; Wang, X.; Roseman, S. The chitin catabolic cascade in the marine bacterium *Vibrio cholerae*: Characterization of a unique chitin oligosaccharide deacetylase. *Glycobiology* **2007**, *17*, 1377–1387. [[CrossRef](#)]
83. Pruzzo, C.; Vezzulli, L.; Colwell, R.R. Global impact of *Vibrio cholerae* interactions with chitin. *Environ. Microbiol.* **2008**, *10*, 1400–1410. [[CrossRef](#)] [[PubMed](#)]
84. Sison-Mangus, M.P.; Jiang, S.; Kudela, R.M.; Mehic, S. Phytoplankton-Associated Bacterial Community Composition and Succession during Toxic Diatom Bloom and Non-Bloom Events. *Front. Microbiol.* **2016**, *7*, 1433. [[CrossRef](#)] [[PubMed](#)]
85. Broza, M.; Gancz, H.; Halpern, M.; Kashi, Y. Adult non-biting midges: Possible windborne carriers of *Vibrio cholerae* non-O1 non-O139. *Environ. Microbiol.* **2005**, *7*, 576–585. [[CrossRef](#)] [[PubMed](#)]
86. Broza, M.; Halpern, M. Chironomid egg masses and *Vibrio cholerae*. *Nature* **2001**, *412*, 40. [[CrossRef](#)] [[PubMed](#)]
87. Ogg, J.E.; Ryder, R.A.; Smith, H.L. Isolation of *Vibrio cholerae* from aquatic birds in Colorado and Utah. *Appl. Environ. Microbiol.* **1989**, *55*, 95–99. [[PubMed](#)]
88. Laviad-Shitrit, S.; Lev-Ari, T.; Katzir, G.; Sharaby, Y.; Izhaki, I.; Halpern, M. Great cormorants (*Phalacrocorax carbo*) as potential vectors for the dispersal of *Vibrio cholerae*. *Sci. Rep.* **2017**, *7*, 7973. [[CrossRef](#)] [[PubMed](#)]
89. Laviad-Shitrit, S.; Izhaki, I.; Arakawa, E.; Halpern, M. Wild waterfowl as potential vectors of *Vibrio cholerae* and *Aeromonas* species. *Trop. Med. Int. Health* **2018**, *23*, 758–764. [[CrossRef](#)]
90. Spira, W.M.; Huq, A.; Ahmed, Q.S.; Saeed, Y.A. Uptake of *Vibrio cholerae* Biotype eltor from Contaminated Water by Water Hyacinth (*Eichornia crassipes*). *Appl. Environ. Microbiol.* **1981**, *42*, 550–553.
91. Feikin, D.R.; Tabu, C.W.; Gichuki, J. Does Water Hyacinth on East African Lakes Promote Cholera Outbreaks? *Am. J. Trop. Med. Hyg.* **2010**, *83*, 370–373. [[CrossRef](#)]
92. Wachsmuth, I.K.; Evins, G.M.; Fields, P.I.; Olsvik, Ø.; Popovic, T.; Bopp, C.A.; Wells, J.G.; Carrillo, C.; Blake, P.A. The Molecular Epidemiology of Cholera in Latin America. *J. Infect. Dis.* **1993**, *167*, 621–626. [[CrossRef](#)]
93. McCarthy, S.A.; Khambaty, F.M. International dissemination of epidemic *Vibrio cholerae* by cargo ship ballast and other nonpotable waters. *Appl. Environ. Microbiol.* **1994**, *60*, 2597–2601. [[PubMed](#)]
94. Rivera, I.N.G.; Souza, K.M.C.; Souza, C.P.; Lopes, R.M. Free-Living and Plankton-Associated Vibrios: Assessment in Ballast Water, Harbor Areas, and Coastal Ecosystems in Brazil. *Front. Microbiol.* **2013**, *3*, 443. [[CrossRef](#)] [[PubMed](#)]
95. Ng, C.; Le, T.H.; Goh, S.G.; Liang, L.; Kim, Y.; Rose, J.B.; Yew-Hoong, K.G. A Comparison of Microbial Water Quality and Diversity for Ballast and Tropical Harbor Waters. *PLoS ONE* **2015**, *10*, e0143123. [[CrossRef](#)] [[PubMed](#)]
96. Kirstein, I.V.; Kirmizi, S.; Wichels, A.; Garin-Fernandez, A.; Erler, R.; Löder, M.; Gerdtts, G. Dangerous hitchhikers? Evidence for potentially pathogenic *Vibrio* spp. on microplastic particles. *Mar. Environ. Res.* **2016**, *120*, 1–8. [[CrossRef](#)]
97. Rodrigues, A.; Oliver, D.M.; McCarron, A.; Quilliam, R.S. Colonisation of plastic pellets (nurdles) by *E. coli* at public bathing beaches. *Mar. Pollut. Bull.* **2019**, *139*, 376–380. [[CrossRef](#)]
98. Yokota, K.; Waterfield, H.; Hastings, C.; Davidson, E.; Kwietniewski, E.; Wells, B. Finding the missing piece of the aquatic plastic pollution puzzle: Interaction between primary producers and microplastics. *Limnol. Oceanogr. Lett.* **2017**, *2*, 91–104. [[CrossRef](#)]
99. Jeuniaux, C.; Voss-Foucart, M.F. Chitin biomass and production in the marine environment. *Biochem. Syst. Ecol.* **1991**, *19*, 347–356. [[CrossRef](#)]

100. Trtanj, J.; Jantarasami, L.; Brunkard, J.; Collier, T.; Jacobs, J.; Lipp, E.; McLellan, S.; Moore, S.; Paerl, H.; Ravenscroft, J.; et al. *Ch. 6: Climate Impacts on Water-Related Illness. The Impacts of Climate Change on Human Health in the United States: A Scientific Assessment*; MFR, U.S. Global Change Research Program: Washington, DC, USA, 2016.
101. Parmesan, C.; Attrill, M. Impacts and effects of ocean warming on human health (disease). In *Explaining Ocean Warming: Causes, Scale, Effects and Consequences*; Laffoley, D., Baxter, J.M., Eds.; IUCN: Gland, Switzerland, 2016; pp. 439–449.
102. Koelle, K. The impact of climate on the disease dynamics of cholera. *Clin. Microbiol. Infect.* **2009**, *15*, 29–31. [[CrossRef](#)]
103. Colwell, R.; Patz, J. *Climate, Infectious Disease and Health: An Interdisciplinary Perspective*; MFR: Washington, DC, USA, 1998.
104. Pascual, M.; Bouma, M.J.; Dobson, A.P. Cholera and climate: Revisiting the quantitative evidence. *Microbes Infect.* **2002**, *4*, 237–245. [[CrossRef](#)]
105. Pascual, M.; Chaves, L.; Cash, B.; Rodó, X.; Yunus, M. Predicting endemic cholera: The role of climate variability and disease dynamics. *Clim. Res.* **2008**, *36*, 131–140. [[CrossRef](#)]
106. Moore, J.K.; Fu, W.; Primeau, F.; Britten, G.L.; Lindsay, K.; Long, M.; Doney, S.C.; Mahowald, N.; Hoffman, F.; Randerson, J.T. Sustained climate warming drives declining marine biological productivity. *Science* **2018**, *359*, 1139–1143. [[CrossRef](#)] [[PubMed](#)]
107. Martinez, P.P.; Reiner, R.C.; Cash, B.A.; Rodó, X.; Mondal, M.S.; Roy, M.; Yunus, M.; Faruque, A.S.G.; Huq, S.; King, A.A.; et al. Cholera forecast for Dhaka, Bangladesh, with the 2015–2016 El Niño: Lessons learned. *PLoS ONE* **2017**, *12*, e0172355. [[CrossRef](#)] [[PubMed](#)]
108. Cash, B.A.; Rodó, X.; Kinter, J.L. Links between Tropical Pacific SST and Cholera Incidence in Bangladesh: Role of the Eastern and Central Tropical Pacific. *J. Clim.* **2008**, *21*, 4647–4663. [[CrossRef](#)]
109. Hashizume, M.; Armstrong, B.; Hajat, S.; Wagatsuma, Y.; Faruque, A.S.G.; Hayashi, T.; Sack, D.A. The Effect of Rainfall on the Incidence of Cholera in Bangladesh. *Epidemiology* **2008**, *19*, 103–110. [[CrossRef](#)] [[PubMed](#)]
110. Martinez-Urtaza, J.; Trinanes, J.; Gonzalez-Escalona, N.; Baker-Austin, C. Is El Niño a long-distance corridor for waterborne disease? *Nat. Microbiol.* **2016**, *1*, 16018. [[CrossRef](#)]
111. Vezzulli, L.; Brettar, I.; Pezzati, E.; Reid, P.C.; Colwell, R.R.; Höfle, M.G.; Pruzzo, C. Long-term effects of ocean warming on the prokaryotic community: Evidence from the vibrios. *ISME J.* **2012**, *6*, 21–30. [[CrossRef](#)]
112. Jacobs, J.; Moore, S.K.; Kunkel, K.E.; Sun, L. A framework for examining climate-driven changes to the seasonality and geographical range of coastal pathogens and harmful algae. *Clim. Risk Manag.* **2015**, *8*, 16–27. [[CrossRef](#)]
113. Sperling, M.; Piontek, J.; Gerdts, G.; Wichels, A.; Schunck, H.; Roy, A.S.; Roche, J.L.; Gilbert, J.; Nissimov, J.I.; Bittner, L.; et al. Effect of elevated CO₂ on the dynamics of particle-attached and free-living bacterioplankton communities in an Arctic fjord. *Biogeosciences* **2013**, *10*, 181–191. [[CrossRef](#)]
114. Riebesell, U.; Aberle-Malzahn, N.; Achterberg, E.P.; Algueró-Muñiz, M.; Alvarez-Fernandez, S.; Arístegui, J.; Bach, L.T.; Boersma, M.; Boxhammer, T.; Guan, W.; et al. Toxic algal bloom induced by ocean acidification disrupts the pelagic food web. *Nat. Clim. Chang.* **2018**, *8*, 1082–1086. [[CrossRef](#)]
115. Beck, L.R.; Lobitz, B.M.; Wood, B.L. Remote sensing and human health: New sensors and new opportunities. *Emerg. Infect. Dis.* **2000**, *6*, 217. [[CrossRef](#)]
116. Lobitz, B.; Beck, L.; Huq, A.; Wood, B.; Fuchs, G.; Faruque, A.S.G.; Colwell, R. Climate and infectious disease: Use of remote sensing for detection of *Vibrio cholerae* by indirect measurement. *Proc. Natl. Acad. Sci. USA* **2000**, *97*, 1438–1443. [[CrossRef](#)] [[PubMed](#)]
117. Tatem, A.J.; Goetz, S.J.; Hay, S.I. Terra and Aqua: New data for epidemiology and public health. *Int. J. Appl. Earth Obs. Geoinf.* **2004**, *6*, 33–46. [[CrossRef](#)] [[PubMed](#)]
118. de Magny, G.C.; Paroissin, C.; Cazelles, B.; de Lara, M.; Delmas, J.F.; Guégan, J.F. Modeling environmental impacts of plankton reservoirs on cholera population dynamics. *ESAIM Proc.* **2005**, *14*, 156–173. [[CrossRef](#)]
119. Finger, F.; Knox, A.; Bertuzzo, E.; Mari, L.; Bompangue, D.; Gatto, M.; Rodriguez-Iturbe, I.; Rinaldo, A. Cholera in the Lake Kivu region (DRC): Integrating remote sensing and spatially explicit epidemiological modeling. *Water Resour. Res.* **2014**, *50*, 5624–5637. [[CrossRef](#)]

120. Sathyendranath, S.; Abdulaziz, A.; Menon, N.; Grinson, G.; Evers-King, H.; Kulk, G.; Colwell, R.; Jutla, A.S.; Platt, T. Building capacity and resilience against diseases transmitted via water under climate perturbations and extreme weather stress. In *Space Capacity Building in the XXI Century*; Ferretti, S., Ed.; Springer Nature: Basel, Switzerland, 2019; Volume 24, p. 14.
121. Konrad, S.; Paduraru, P.; Romero-Barrios, P.; Henderson, S.B.; Galanis, E. Remote sensing measurements of sea surface temperature as an indicator of *Vibrio parahaemolyticus* in oyster meat and human illnesses. *Environ. Health* **2017**, *16*, 92. [[CrossRef](#)]
122. Xu, M.; Cao, C.; Wang, D.; Kan, B. Identifying Environmental Risk Factors of Cholera in a Coastal Area with Geospatial Technologies. *Int. J. Environ. Res. Public Health* **2015**, *12*, 354–370. [[CrossRef](#)]
123. Jutla, A.; Akanda, A.S.; Huq, A.; Faruque, A.S.G.; Colwell, R.; Islam, S. A water marker monitored by satellites to predict seasonal endemic cholera. *Remote Sens. Lett.* **2013**, *4*, 822–831. [[CrossRef](#)]
124. Jutla, A.S.; Akanda, A.S.; Islam, S. Satellite Remote Sensing of Space-Time Plankton Variability in the Bay of Bengal: Connections to Cholera Outbreaks. *Remote Sens. Environ.* **2012**, *123*, 196–206. [[CrossRef](#)]
125. Nkoko, D.; Giraudoux, P.; Plisnier, P.D.; Tinda, A.; Piarroux, M.; Sudre, B.; Horion, S.; Tamfum, J.J.; Ilunga, B.; Piarroux, R. Dynamics of Cholera Outbreaks in Great Lakes Region of Africa, 1978–2008. *Emerg. Infect. Dis.* **2011**, *17*, 2026. [[CrossRef](#)]
126. Emch, M.; Yunus, M.; Escamilla, V.; Feldacker, C.; Ali, M. Local population and regional environmental drivers of cholera in Bangladesh. *Environ. Health* **2010**, *9*, 2. [[CrossRef](#)]
127. Ford, T.E. Using Satellite Images of Environmental Changes to Predict Infectious Disease Outbreaks. *Emerg. Infect. Dis.* **2009**, *15*, 1341–1346. [[CrossRef](#)] [[PubMed](#)]
128. Mendelsohn, J.; Dawson, T. Climate and cholera in KwaZulu-Natal, South Africa: The role of environmental factors and implications for epidemic preparedness. *Int. J. Hyg. Environ. Health* **2008**, *211*, 156–162. [[CrossRef](#)] [[PubMed](#)]
129. Phillips, A.M.B.; DePaola, A.; Bowers, J.; Ladner, S.; Grimes, D.J. An Evaluation of the Use of Remotely Sensed Parameters for Prediction of Incidence and Risk Associated with *Vibrio parahaemolyticus* in Gulf Coast Oysters (*Crassostrea virginica*). *J. Food Prot.* **2007**, *70*, 879–884. [[CrossRef](#)] [[PubMed](#)]
130. Sathyendranath, S.; Brewin, R.J.W.; Brockmann, C.; Brotas, V.; Calton, B.; Chuprin, A.; Cipollini, P.; Couto, A.B.; Dingle, J.; Doerffer, R.; et al. An Ocean-Colour Time Series for Use in Climate Studies: The Experience of the Ocean-Colour Climate Change Initiative (OC-CCI). *Sensors* **2019**, *19*, 4285. [[CrossRef](#)]
131. Akanda, A.S.; Jutla, A.S.; Gute, D.M.; Sack, R.B.; Alam, M.; Huq, A.; Colwell, R.R.; Islam, S. Population Vulnerability to Biannual Cholera Outbreaks and Associated Macro-Scale Drivers in the Bengal Delta. *Am. J. Trop. Med. Hyg.* **2013**, *89*, 950–959. [[CrossRef](#)]
132. Bouma, M.J.; Pascual, M. Seasonal and interannual cycles of endemic cholera in Bengal 1891–1940 in relation to climate and geography. *Hydrobiologia* **2001**, *460*, 147–156. [[CrossRef](#)]
133. CEOS EO HANDBOOK. Available online: <http://eohandbook.com/sdg/> (accessed on 30 September 2019).
134. Groom, S.; Sathyendranath, S.; Ban, Y.; Bernard, S.; Brewin, R.; Brotas, V.; Brockmann, C.; Chauhan, P.; Choi, J.; Chuprin, A.; et al. Satellite Ocean Colour: Current Status and Future Perspective. *Front. Mar. Sci.* **2019**, *6*, 485. [[CrossRef](#)]
135. Donlon, C.; Berruti, B.; Buongiorno, A.; Ferreira, M.H.; Féménias, P.; Frerick, J.; Goryl, P.; Klein, U.; Laur, H.; Mavrocordatos, C.; et al. The Global Monitoring for Environment and Security (GMES) Sentinel-3 mission. *Remote Sens. Environ.* **2012**, *120*, 37–57. [[CrossRef](#)]
136. Liardon, J.L.; Hostettler, L.; Zulliger, L.; Kangur, K.; Shaik, N.; Barry, D.A. Lake Imaging and Monitoring Aerial Drone. *HardwareX* **2018**, *3*, 146–159. [[CrossRef](#)]
137. Wu, J.L.; Ho, C.R.; Huang, C.C.; Srivastav, A.L.; Tzeng, J.H.; Lin, Y.T. Hyperspectral Sensing for Turbid Water Quality Monitoring in Freshwater Rivers: Empirical Relationship between Reflectance and Turbidity and Total Solids. *Sensors* **2014**, *14*, 22670–22688. [[CrossRef](#)]
138. Kisevic, M.; Morovic, M.; Andricevic, R. The use of hyperspectral data for evaluation of water quality parameters in the River Sava. *Fresenius Environ. Bull.* **2016**, *25*, 4814–4822.
139. Bidigare, R.R.; Ondrusek, M.E.; Morrow, J.H.; Kiefer, D.A. In-vivo absorption properties of algal pigments. 1990, Volume 1302, pp. 290–302. Available online: https://www.researchgate.net/publication/252465392_In-vivo_absorption_properties_of_algal_pigments (accessed on 30 September 2019).

140. Trees, C.C.; Clark, D.K.; Bidigare, R.R.; Ondrusek, M.E.; Mueller, J.L. Accessory pigments versus chlorophyll a concentrations within the euphotic zone: A ubiquitous relationship. *Limnol. Oceanogr.* **2000**, *45*, 1130–1143. [[CrossRef](#)]
141. Sathyendranath, S.; Cota, G.; Stuart, V.; Maass, H.; Platt, T. Remote sensing of phytoplankton pigments: A comparison of empirical and theoretical approaches. *Int. J. Remote Sens.* **2001**, *22*, 249–273. [[CrossRef](#)]
142. Brewin, R.J.W.; Sathyendranath, S.; Hirata, T.; Lavender, S.J.; Barciela, R.M.; Hardman-Mountford, N.J. A three-component model of phytoplankton size class for the Atlantic Ocean. *Ecol. Model.* **2010**, *221*, 1472–1483. [[CrossRef](#)]
143. Brewin, R.J.W.; Dall’Olmo, G.; Sathyendranath, S.; Hardman-Mountford, N.J. Particle backscattering as a function of chlorophyll and phytoplankton size structure in the open-ocean. *Opt. Express* **2012**, *20*, 17632–17652. [[CrossRef](#)]
144. Brewin, R.J.W.; Sathyendranath, S.; Jackson, T.; Barlow, R.; Brotas, V.; Airs, R.; Lamont, T. Influence of light in the mixed-layer on the parameters of a three-component model of phytoplankton size class. *Remote Sens. Environ.* **2015**, *168*, 437–450. [[CrossRef](#)]
145. Brewin, R.J.W.; Morán, X.A.G.; Raitsos, D.E.; Gittings, J.A.; Calleja, M.L.; Viegas, M.; Ansari, M.I.; Al-Otaibi, N.; Huete-Stauffer, T.M.; Hoteit, I. Factors Regulating the Relationship Between Total and Size-Fractionated Chlorophyll-a in Coastal Waters of the Red Sea. *Front. Microbiol.* **2019**, *10*, 1964. [[CrossRef](#)]
146. Alvain, S.; Moulin, C.; Dandonneau, Y.; Bréon, F.M. Remote sensing of phytoplankton groups in case 1 waters from global SeaWiFS imagery. *Deep Sea Res. Part Oceanogr. Res.* **2005**, *52*, 1989–2004. [[CrossRef](#)]
147. Alvain, S.; Moulin, C.; Dandonneau, Y.; Loisel, H. Seasonal distribution and succession of dominant phytoplankton groups in the global ocean: A satellite view. *Glob. Biogeochem. Cycles* **2008**, *22*. [[CrossRef](#)]
148. Alvain, S.; Loisel, H.; Dessailly, D. Theoretical analysis of ocean color radiances anomalies and implications for phytoplankton groups detection in case 1 waters. *Opt. Express* **2012**, *20*, 1070–1083. [[CrossRef](#)] [[PubMed](#)]
149. Réve-Lamarche, A.H.; Alvain, S.; Racault, M.F.; Dessailly, D.; Guiselin, N.; Jamet, C.; Vantrepotte, V.; Beaugrand, G. Estimation of the Potential Detection of Diatom Assemblages Based on Ocean Color Radiance Anomalies in the North Sea. *Front. Mar. Sci.* **2017**, *4*, 408. [[CrossRef](#)]
150. Sathyendranath, S.; Watts, L.; Devred, E.; Platt, T.; Caverhill, C.; Maass, H. Discrimination of diatoms from other phytoplankton using ocean-colour data. *Mar. Ecol. Prog. Ser.* **2004**, *272*, 59–68. [[CrossRef](#)]
151. Racault, M.F.; Le Quéré, C.; Buitenhuis, E.; Sathyendranath, S.; Platt, T. Phytoplankton phenology in the global ocean. *Ecol. Indic.* **2012**, *14*, 152–163. [[CrossRef](#)]
152. Racault, M.F.; Raitsos, D.E.; Berumen, M.L.; Brewin, R.J.W.; Platt, T.; Sathyendranath, S.; Hoteit, I. Phytoplankton phenology indices in coral reef ecosystems: Application to ocean-color observations in the Red Sea. *Remote Sens. Environ.* **2015**, *160*, 222–234. [[CrossRef](#)]
153. Racault, M.F.; Sathyendranath, S.; Menon, N.; Platt, T. Phenological Responses to ENSO in the Global Oceans. *Surv. Geophys.* **2017**, *38*, 277–293. [[CrossRef](#)]
154. Cole, H.S.; Henson, S.; Martin, A.P.; Yool, A. Basin-wide mechanisms for spring bloom initiation: How typical is the North Atlantic? *ICES J. Mar. Sci.* **2015**, *72*, 2029–2040. [[CrossRef](#)]
155. Sallée, J.B.; Llorc, J.; Tagliabue, A.; Lévy, M. Characterization of distinct bloom phenology regimes in the Southern Ocean. *ICES J. Mar. Sci.* **2015**, *72*, 1985–1998. [[CrossRef](#)]
156. Platt, T.; Sathyendranath, S. Oceanic Primary Production: Estimation by Remote Sensing at Local and Regional Scales. *Science* **1988**, *241*, 1613–1620. [[CrossRef](#)]
157. Sathyendranath, S.; Stuart, V.; Nair, A.; Oka, K.; Nakane, T.; Bouman, H.; Forget, M.H.; Maass, H.; Platt, T. Carbon-to-chlorophyll ratio and growth rate of phytoplankton in the sea. *Mar. Ecol. Prog. Ser.* **2009**, *383*, 73–84. [[CrossRef](#)]
158. Martinez-Vicente, V.; Dall’Olmo, G.; Tarran, G.; Boss, E.; Sathyendranath, S. Optical backscattering is correlated with phytoplankton carbon across the Atlantic Ocean. *Geophys. Res. Lett.* **2013**, *40*, 1154–1158. [[CrossRef](#)]
159. Kostadinov, T.S.; Milutinović, S.; Marinov, I.; Cabré, A. Carbon-based phytoplankton size classes retrieved via ocean color estimates of the particle size distribution. *Ocean Sci.* **2016**, *12*, 561–575. [[CrossRef](#)]
160. Roy, S.; Sathyendranath, S.; Platt, T. Size-partitioned phytoplankton carbon and carbon-to-chlorophyll ratio from ocean colour by an absorption-based bio-optical algorithm. *Remote Sens. Environ.* **2017**, *194*, 177–189. [[CrossRef](#)]

161. Dogliotti, A.I.; Ruddick, K.G.; Nechad, B.; Doxaran, D.; Knaeps, E. A single algorithm to retrieve turbidity from remotely-sensed data in all coastal and estuarine waters. *Remote Sens. Environ.* **2015**, *156*, 157–168. [[CrossRef](#)]
162. Stramski, D.; Reynolds, R.A.; Babin, M.; Kaczmarek, S.; Lewis, M.R.; Röttgers, R.; Sciandra, A.; Stramska, M.; Twardowski, M.S.; Franz, B.A.; et al. Relationships between the surface concentration of particulate organic carbon and optical properties in the eastern South Pacific and eastern Atlantic Oceans. *Biogeosciences* **2008**, *5*, 171–201. [[CrossRef](#)]
163. Evers-King, H.; Martinez-Vicente, V.; Brewin, R.J.W.; Dall’Olmo, G.; Hickman, A.E.; Jackson, T.; Kostadinov, T.S.; Krasemann, H.; Loisel, H.; Röttgers, R.; et al. Validation and Intercomparison of Ocean Color Algorithms for Estimating Particulate Organic Carbon in the Oceans. *Front. Mar. Sci.* **2017**, *4*, 251. [[CrossRef](#)]
164. Gordon, H.R.; Boynton, G.C.; Balch, W.M.; Groom, S.B.; Harbour, D.S.; Smyth, T.J. Retrieval of coccolithophore calcite concentration from SeaWiFS Imagery. *Geophys. Res. Lett.* **2001**, *28*, 1587–1590. [[CrossRef](#)]
165. Balch, W.M.; Gordon, H.R.; Bowler, B.C.; Drapeau, D.T.; Booth, E.S. Calcium carbonate measurements in the surface global ocean based on Moderate-Resolution Imaging Spectroradiometer data. *J. Geophys. Res. Oceans* **2005**, *110*. [[CrossRef](#)]
166. Smyth, T.J.; Tyrrell, T.; Tarrant, B. Time series of coccolithophore activity in the Barents Sea, from twenty years of satellite imagery. *Geophys. Res. Lett.* **2004**, *31*. [[CrossRef](#)]
167. Moore, T.S.; Dowell, M.D.; Franz, B.A. Detection of coccolithophore blooms in ocean color satellite imagery: A generalized approach for use with multiple sensors. *Remote Sens. Environ.* **2012**, *117*, 249–263. [[CrossRef](#)]
168. Lee, Z.; Carder, K.L.; Arnone, R.A. Deriving inherent optical properties from water color: A multiband quasi-analytical algorithm for optically deep waters. *Appl. Opt.* **2002**, *41*, 5755–5772. [[CrossRef](#)] [[PubMed](#)]
169. Maritorena, S.; Siegel, D.A.; Peterson, A.R. Optimization of a semianalytical ocean color model for global-scale applications. *Appl. Opt.* **2002**, *41*, 2705–2714. [[CrossRef](#)] [[PubMed](#)]
170. Werdell, P.J.; Franz, B.A.; Bailey, S.W.; Feldman, G.C.; Boss, E.; Brando, V.E.; Dowell, M.; Hirata, T.; Lavender, S.J.; Lee, Z.; et al. Generalized ocean color inversion model for retrieving marine inherent optical properties. *Appl. Opt.* **2013**, *52*, 2019–2037. [[CrossRef](#)] [[PubMed](#)]
171. Doney, S.C. Plankton in a warmer world. *Nature* **2006**, *444*, 695–696. [[CrossRef](#)]
172. Ali, M.; Nelson, A.R.; Lopez, A.L.; Sack, D.A. Updated Global Burden of Cholera in Endemic Countries. *PLoS Negl. Trop. Dis.* **2015**, *9*, e0003832. [[CrossRef](#)]
173. Scharlemann, J.P.W.; Mant, R.C.; Balfour, N.; Brown, C.; Burgess, N.D.; Guth, M.; Ingram, D.J.; Lane, R.; Martin, J.; Wicander, S.; et al. Global Goals Mapping: The Environment-Human Landscape. Available online: <http://www.nerc.ac.uk/research/partnerships/international/overseas/tase/mapping/> (accessed on 30 September 2019).
174. Brewin, R.J.W.; Brewin, T.G.; Phillips, J.; Rose, S.; Abdulaziz, A.; Wimmer, W.; Sathyendranath, S.; Platt, T. A Printable Device for Measuring Clarity and Colour in Lake and Nearshore Waters. *Sensors* **2019**, *19*, 936. [[CrossRef](#)]
175. Akanda, A.S.; Aziz, A.; Jutla, A.; Huq, A.; Alam, M.; Asham, G.U.; Colwell, R.R. Satellites and Cell Phones Form a Cholera Early-Warning System. *Eos Trans. Am. Geophys. Union* **2018**, *99*. [[CrossRef](#)]
176. Finger, F.; Genolet, T.; Mari, L.; de Magny, G.C.; Manga, N.M.; Rinaldo, A.; Bertuzzo, E. Mobile phone data highlights the role of mass gatherings in the spreading of cholera outbreaks. *Proc. Natl. Acad. Sci. USA* **2016**, *113*, 6421–6426. [[CrossRef](#)]
177. Abubakar, A.; Azman, A.S.; Rumunu, J.; Ciglenecki, I.; Helderma, T.; West, H.; Lessler, J.; Sack, D.A.; Martin, S.; Perea, W.; et al. The First Use of the Global Oral Cholera Vaccine Emergency Stockpile: Lessons from South Sudan. *PLoS Med.* **2015**, *12*, e1001901. [[CrossRef](#)]

